Contract DAJA5A-93-C-0010

Final Report, February 1995

Michael H Abraham, Jenik Andonian-Haftvan and Chau My Du

The Department of Chemistry, University College London,

20 Gordon Street, London, WC1H 0AJ, UK

In this final report we set out all the methods that have been used, and all the results that have been obtained, on this contract, in order that the report should be completely self-contained. We deal first with the theoretical background of the linear free energy relationships that we use to analyse the results, and then we discuss the various areas of work with which we have been concerned. A Table of Contents is on page 2.

Table of Contents

1. The Linear Free Energy Equation

Our use of linear free energy equations (LFERs) to characterize liquids and solids, is based on two equations that include various solute properties necessary for a general analysis of physicochemical phenomena [1,2]. These two equations have been constructed for processes in which a number of solutes is studied in a fixed solvent (or phase) system. Hence the properties of the solvent or the solid phase remain constant, and only the properties of the solutes vary. It is these solute properties that are used as the explanatory variables, or descriptors, in the two LFERS.

$$\log SP = c + r.R_2 + s.\pi^H_2 + a.\Sigma\alpha^H_2 + b.\Sigma\beta^H_2 + l.\log L^{16} \qquad (1)$$

$$\log SP = c + r.R_2 + s.\pi^H_2 + a.\Sigma\alpha^H_2 + b.\Sigma\beta^H_2 + v.V_x \qquad (2)$$

In these equations, SP is some property of a series of solutes in a given system, and the explanatory variables, or descriptors, are solute properties as follows.[1,2] R_2 is an excess molar refraction; π^H_2 is the solute dipolarity/ polarizability, it being not possible to devise descriptors for these properties separately; $\Sigma\alpha^H_2$ is the solute overall or effective hydrogen-bond acidity; $\Sigma\beta^H_2$ is the solute overall or effective hydrogen-bond basicity; $\log L^{16}$ is a descriptor defined [3] as the solute gas-liquid partition coefficient on hexadecane at 298K; V_x is the McGowan characteristic volume.[4]

Eq(1) and eq (2) are solved by the method of multiple linear regression analysis (MLRA), to yield the various coefficients in the equations. In carrying out the multiple regression a reasonable number of data points is required, if there are too few data points the regression may not be reliable. As a general rule, a minimum of five solutes per variable is taken, although it is preferable to have more. Other important points to take note of when carrying out MLRA, are that the set of data used should give a wide range of parameters , and that the set of solutes selected should not lead to multicolinearity of parameters. Not all the descriptors in eq(1) or eq(2) may be significant, and statistical procedures using the t-test or the F-statistic are employed as tests of significance.

The first four descriptors in eq(1) and eq(2) can be regarded as measures of the propensity of a solute to undergo various solute-solvent interactions, all of which are energetically favorable, ie exoergic. The $\log L^{16}$ and the V_x descriptor model a combination of an endoergic cavity effect and an exoergic general dispersion interaction between solute and system. Because the descriptors in eq(1) and eq(2) refer to rather specific interactions, the coefficients (or constants) in eq(1) and eq(2) will contain information on the particular solvent phase or solid phase in question. The r-constant, although not usually very important, is a measure of the phase polarizability, the s-constant measures the phase dipolarity/polarizability, the

a-constant is a measure of the phase hydrogen-bond basicity (because an acidic solute will interact with a basic phase), and the b-constant is a measure of the phase acidity. Both the l-constant and the v-constant are measures of the phase hydrophobicity. Of course, if the equations are applied to distribution between two phases, the constants will then refer to differences between the phases concerned. Eq(1) is usually the better equation to use for gas-condensed phase processes, and this is the equation that we shall normally use. Eq(3) is more useful for processes such as the distribution of solutes between two solvent phases, but in the present work, eq(3) is only useful in the determination of solute descriptors.

There is no difficulty over the R_2 and V_x descriptors. The former can be obtained from refractive index measurements on liquids, and can easily be estimated for gases and solids, and the latter can simply be calculated. The $\log L^{16}$ descriptor is only applicable to solutes that are not too involatile, and can be obtained from gas-liquid chromatographic (GLC) measurements. For many aliphatic compounds, Havelec and Sevcik [5] have shown that $\log L^{16}$ can be estimated through a group additivity scheme. We are therefore left with three other descriptors that have to be determined, π^H_2, $\Sigma\alpha^H_2$ and $\Sigma\beta^H_2$. For volatile solutes, the π^H_2 descriptor can be obtained by gas-liquid chromatography (GLC) on a polar, nonacidic, stationary phase. For volatile solutes, the GLC method can in principle be used to obtain $\Sigma\alpha^H_2$ and $\Sigma\beta^H_2$ values as well, but a better method is to use partition coefficients for various water-solvent systems. The method is based [6] on the construction of LFERs using eq(2), where logSP is logP, a partition coefficient in a given system. For example, the water-cyclohexane partition coefficient, as logPcyc can be correlated [7] with the descriptors in eq(2) to yield,

$$\log Pcyc = 0.13 + 0.82\ R_2 - 1.73\ \pi^H_2 - 3.78\ \Sigma\alpha^H_2 - 4.91\ \Sigma\beta^H_2 + 4.65\ V_x \qquad (3)$$

Similar equations can be constructed [6,7] for the correlation of numerous partitions. In principle, logP values in three water-solvent systems for a given solute could be used to calculate the three unknown descriptors through three simultaneous equations. But in practice, this method will only work if the three logP equations have quite diferent coefficients in the three descriptor terms. Our preferred method is to use logP values for as many systems as possible, and then to calculate the set of descriptors that best describes the logP values.

In practice, the method we use to obtain descriptors is mostly based on a combination of eq(1) and eq(2), using as much data as possible. Most of the experimental data needed in eq(1), we have detemined in this work, but nearly all the partition coefficient data needed in eq(2) has been taken from the literature.[8]

2. Inverse Gas-Chromatography

The general objective of this type of work is to understand the factors that govern solubility processes between solvents and solutes, and the interactions on solid surfaces with gaseous molecules. This ultimately leads to general models of solubility and sorption that can quantitatively describe the various processes that occur.

The present work involves the characterising of polymers and solids, in terms of their dipolarity/polarisability, hydrogen-bond capability, and dispersion interaction towards gaseous solutes. The usefulness of these polymers and solids is based on their ability to distinguish between probe solutes, and hence their ability to dissolve (and be dissolved by) various compounds.

The method of characterisation involves measuring solubiliies or sorption properties, (SP), for a series of solutes on a given liquid or solid phase. These SP values are then analysed using the LFER, eq(1), by the method of multiple linear regression analysis (MLRA), as described above.

3. Gas-solid Adsorption

3.1 Introduction

IGC is increasingly used to investigate adsorbents, and is the chosen method in this work. From the peak shape, the gas-solid adsorption isotherm can be obtained by the method of elution by characteristic point.[9] However, the concentration range for adsorption work is very much smaller than in gas-liquid systems for the isotherm to be linear. So the concentration of sample used here though very small could be high enough to enter the non-linear region of the isotherm, which may be why some of the adsorbates show non-linear adsorption isotherms. The reason for non-linear behaviour is due to an increasing number of active sites being occupied by adsorbents relative to the concentration at equilibrium and causes the diversion of linearity relationship in the plot of C_s against C_g. Here, C_s is the concentration of the sorbed probe in the solid phase, and C_g is the concentration of the probe in the gas-phase. The equilibrium relationship between a solid sorbent and a gaseous adsorbate at constant temperature is called an adsorption isotherm.

There are a number of methods available to calculate adsorption isotherms, namely, frontal analysis (FA), frontal analysis by characteristic point (FACP), and elution by characteristic point (ECP). Both FA and FACP involve analysis of the frontal boundary or break through curve, while ECP involves analysis of the elution boundary of the chromatographic peak. In ECP, the isotherm can be obtained from a single chromatographic peak, and is the technique adopted. A full description of this technique is given by Conder and Young.[9] The ECP method involves the injection of a sample into a carrier gas stream which is passing through a packed column. The chromatographic peak can then be analysed to give the adsorption isotherm and the partition

constant, from the linear, infinite dilution region of the isotherm. The disadvantage of ECP is that results can be significantly affected by non-ideal effects due mainly to the random nature of diffusion which leads to band spreading. Thus, it is necessary to correct the peak to eliminate such effect before the isotherm is calculated.

3.2 Diffusion correction

The simplest assumption that can be made is that the rate of broadening by diffusion is equal on both sides of the peak. Then the corrected curve lies halfway between the front and rear sides of the peak.

3.3 Adsorption isotherm

There are several types of isotherm, which for gases on solids can mostly be described by a Langmuir isotherm. This isotherm theory of Langmuir postulates that the adsorption equilibrium increases relatively rapidly with pressure or adsorbate concentration and then gradually falls as the adsorbent surface is covered with a mono-layer of gas molecules. At high pressure the isotherm levels off to some saturation value. The Langmuir isotherm allows the surface area of the adsorbent to be found as shown

$$C_s = C_{sm}.K.C_g/(1 + K.C_s) \qquad (4)$$

Here C_{sm} and K are constants and are characteristic of the system under consideration and are evaluatated from experimental data; C_{sm} is the amount of the gas required to cover a monolayer surface of solid and K is the adsorption or partition constant. The term $1/C_{sm}.K$ is the Henry's constant K^H_c , and is obtained by measuring the slope of the plot of C_s against C_g as C_g -- 0. C_s and C_g are the equilibrium concentration of the adsorbate in the solid and gas phase respectively. The Henry's constant K^H_p can be found by plotting C_s against P_2 as P_2 -- 0; P_2 is the equilibrium partial pressure of the adsorbate. For adsorption on a homogeneous surface at a sufficiently low concentration, such that all adsorbate molecules are isolated from each other, the equilibrium relationship between gas phase and adsorbent is constant over a range of concentration, known as the 'Henry's region'. This linear relationship between P_2 or C_g is known as Henry's law, by analogy with the limiting behaviour of the solubility of gases in liquids. The constant of proportionality is refered to as the partition constant. The equations are:

$$(C_s/P_2) \text{ as } P_2 \text{-- } _0 = K_p = 1/K^H_p \qquad (5)$$

$$(C_s/C_g) \text{ as } Cg \text{-- } _0 = K_c = 1/K^H_c \qquad (6)$$

Where the partition is the reciprocal of the Henry's constant. The units of Kp are [g/g]/atm, and the units of Kc are [g/g]/[g/l]. Eqn (4) can be rearranged to give equation (7);

$$\frac{C_g}{C_s} = \frac{1}{C_{sm}.K} + \frac{C_g}{C_{sm}} \qquad (7)$$

Therefore a plot of C_g/C_s against C_g will have a slope of $(1/C_{sm})$ and an intercept of $(1/C_{sm}.K)$. In principle, values of the slope and intercept may be combined to give the parameter K, but in practice it is not very accurate to use the intercept of this plot to obtain $C_{sm}.K$ (K_c or K_p). A better method is to use a plot C_s against C_g at low partial pressure to obtain K_c, and to combine the value of $C_{sm}.K$ thus found with the value of C_{sm} from the C_g/C_s against C_g plot, to obtain K. It should be noted that although C_{sm} and K are interesting parameters, it is the combined parameter $C_{sm}.K$, or K_c, that reflects the adsorbance of the solute gas or vapour at low concentrations, or similarly K_p at low partial pressures. P_2 and C_g are related by equation (8),

$$P_2 = C_g.R.T/M_2 \qquad (8)$$

Where R is the gas constant, T is the temperature in degrees Kelvin and M_2 is the molecular weight of the adsorbate being studied in grams.

In the elution by the characteristic point method (ECP), sometimes known as the peak profile method, the chromatographic peak observed on injection of a solute is corrected for diffusion and baseline drift. Then a series of areas A^h corresponding to the deflection of the recorder pen, h, can be obtained. C_s is calculated from the area on the chart recorder, (A^h), and C_g, from the recorder pen deflection, h, using known equations. The area, A^h, is proportional to the volume of carrier gas required to elute the adsorbate (at the point on the elution curve at height, h, this is the so called characteristic point), which in turn is proportional to the time spent in the adsorbent, C_s, i.e the concentration in the adsorbent. The pen deflection, h, is proportional to the number of adsorbate molecules passing through the detector at that particular moment (assuming detector linearity with the concentrations studied), which is proportional to the concentration in the gas phase, C_g, or the partial pressure, P_2. Then C_g and C_s are given by,

$$C_s = A^h/S.W_1 \qquad (9)$$

$$C_g = h.Q/F.S \qquad (10)$$

Where S is the sensitivity, defined as the area under the uncorrected peak divided by the amount of sample injected, W_1 is the active weight of adsorbent (i.e the dry weight after purging in gram), Q is the chart recorder speed, and F is the carrier gas flow rate (l/sec) at the column temperature, T (K). The isotherm is calculated using equations (9) and (10), from points on the appropriate boundary (i.e the diffuse boundary following the sharp front boundary). From the ratio of A^h/h, values of C_s/P_2 or C_s/C_g are calculated via equations (11) and (12) respectively. R, the gas constant is taken as $8.2056*10^{-2}$ $l.atm.mol^{-1}deg^{-1}$. (Note that equations (9) and (10) are simply related by eq(8).

$$C_s/P_2 = A^h.F.M_2/(h.W_1.Q.R.T) \qquad (11)$$

$$C_s/Cg = A^h.F/(h.W_1.Q) \qquad (12)$$

Data are collected using an on-line personal computer and an analog digital converter. A program specifically written to recalculate the chromatographic peak data into C_s, C_g and P_2 values can be used to plot isotherms if required. The program also obtains the limiting values of K_c and K_p as defined by eq(5) and eq(6); these are characteristic constants of adsorbate on the adsorbent studied. For the calculation of the partition constants at infinite dilution, the measured flow rate, F_w, is corrected to the actual flow rate, F_c, using eq(13)

$$F_c = F_w.C \qquad (13)$$

Here C is a system constant that depends upon the column properties such as temperature and pressure drop. The pressure drop across the column is the pressure difference between the inlet and outlet of the column and is calculated by using eq(14),

$$J^2_3 = \frac{3\,[(P_i/P_o)^2 - 1]}{2\,[(P_i/P_o)^3 - 1]} \qquad (14)$$

Here J^2_3 is the pressure correction factor, where P_i and P_o are the inlet and outlet pressures. Further corrections are made for the differences between the temperatures of the flow meter (T_w) and the column (T_c), and for the vapour pressure of water above the soap solution in the flow meter (P_w). A full prescription for correcting the flow rate is given by eq(15),

$$F_c = J^2_3.F_w.(P_o - P_w).T_c/(P_o.T_w) \qquad (15)$$

3.4 Experimental discussion

Determination of optimum column size

The optimum column size is that column size which gives correct partition constants for a range of adsorbates with an acceptable time of elution . If the column is too short the adsorbate is not equilibrated and the partition constants will not be correct. If the column is too long the elution time will be very long and this could result in very broad elution boundaries. As these approach the partition region they may be very close to the baseline and thus the signal:noise ratio is small and introduces large errors. Generally, the type of column used is 2 - 3 cm in diameter and the length used depends on the type of adsorbent. For very strong adsorbents, a 2 cm diameter column size is used. For normal or weak adsorbents, then a 3 cm column size is used, as a wider diameter column reduces Eddy diffusion, and pressue drp across a column.

Determination of optimum flow rate

Various flow rates were used in order to find the Height Equivalent to a Theoretical Plate (HETP). It was found that flow rates about 40 - 60 ml/min had acceptable plate heights. However, for small size adsorbates used on Buckminster fullerene, C_{60}, which is a weak adsorbent, a slower flow rate was neccessary, viz

20 ml/min. Otherwise these adsorbates would not stay in the column long enough to interact with the adsorbent, i.e would not be properly equilibrated.

Injection Temperature

An injection temperature of 350K was used to volatalise solutes, although the majority of the solutes injected were gases, because only a small quantity of solute was required.

Adsorbate standard

A standard (n-decane) was chosen so as to give a reasonable elution time, and was injected very frequently to ensure that the adsorbent had the same behaviour after other adsorbates were injected, i.e the surface of the adsorbent was free from previous adsorbates. If the standard elution time was not reproducible, then it was necessary to flush the column out with carrier gas for some time, usually at least 24 hours.

Column conditioning

It was essential to condition the packed column before starting to carry out adsorption studies to remove any impurities on the surface of the adsorbent. Conditioning of the column involved purging with carrier gas for 24 hours. The conditioning temperature depended on the type of adsorbent, so for very strong adsorbents, the conditioning temperature used was 470K, and for weak adsorbents a lower temperature was used. The fullerene column was conditioned at 470K for 24 hours with a continous flow of helium, the carrier gas used. The column was reweighed after being conditioned, and the weight of post conditioned adsorbent was the weight used for any calculations.

Data collection

The peak data was collected into the memory of a PC by a commercial program, Unkelscope and an analog digital converter in the form of an ASCII file. A supplementary program was written to process the collected adsorption data in order to generate partition constants, in terms of concentration as ($\log K_c$) and in terms of partial pressure as ($\log K_p$).

Adsorption program

Before the partition constants can be obtained from an adsorbate peak, a number of corrections and calculations are required,

a) Correction for baseline drift by generating a new baseline, relative to zero, and then correcting the points on the peak so that they are relative to this new baseline. The end result is that the points on the elution boundary are derived from a constant 'backgound' voltage or baseline. Baseline drift is a common problem when adsorbates have long retention times.

b) The finding of the peak retention time and consequently the retention volume.

c) The correction of values in (b) for pressure drop across the column, gas hold up time, variations in atmospheric pressure, flow rate, flow meter temperature variations, and active weight of adsorbent in the column, in order to obtain a value for the specific retention volume (V_G).

d) Correction for diffusion, by subtracting the diffusion at the front boundary from the elution boundary. Correction is necessary, because the front profile of the peak obtained is not sharp but diffuse, due to band spreading.

e) The calculation of pairs of values for C_s-C_g and C_s-P_2.

f) The calculation of $\log K_c$ and $\log K_p$ via a least squares straight line plot using the values in (e).

Use of a chart recorder

It was found that the precision of elution time measurements made with the acquisition software was not as good as the corresponding measurements using a chart recorder. The reason for this is the slow response time of chart recorders. The slow response time of chart recorders compared with modern on line computers has been found to be advantageous when determining elution times. All signals are subject to mains and other electrical interferences. The 'mains' noise does not affect the chart recorder as it is designed to record changes in the overall signal received, and hence rapid periodic oscillations such as 'mains' noise causing no overall change are not recorded. The on-line computer is, however, capable of recording all these oscillations and consequently the signal is noisier and elution times are much more difficult to observe. Thus elution times were recorded with both an on-line computer and a chart recorder monitoring the same signal.

3.5 Buckminsterfullerene

In order to set up the adsorption equipment, and to ensure that both apparatus and the data aquisition system were operative, considerable preliminary studies were necessary. It was felt that it would be useful to carry out such studies with an adsorbent that was not very active, and so Buckminsterfullerene was chosen as an interesting adsorbent to use for this preliminary work. This carbon adsorption is a truncated icosahedral cage structure [10] of formula C_{60}, comprising mainly six-membered rings with a few five-membered rings that help to close the cage into a ball structure. The sample used was obtained from Polygon Enterprises, Waco, Texas, USA, and comprised about 85% C_{60}, the remainder being mostly C_{70}.

The fullerene was sieved at 20-30 mesh size and packed into a column 2.0mm in width and 10.5cm in length, with a post-conditioed weight of 0.1383g. Data were obtained for 22 solutes at 298K, covering a reasonably wide range. It was not possible to study small adsorbents, because of non-equilibration on the adsorbate column. Results are in Table 1, and were analysed using the general eq(1), as outlined above. The

following equations were obtained;

$$\log K_c = -1.580 - 0.237\ R_2 + 0.721\ \pi^H_2 + 1.041\ \Sigma\alpha^H_2 + 0.477\ \log L^{16} \quad (16)$$

$$n = 22, \quad r = 0.9506, \quad sd = 0.124, \quad F = 39.8$$

$$\log K_p = -1.093 + 0.576\ \pi^H_2 + 0.596\ \Sigma\alpha^H_2 + 0.549\ \log L^{16} \quad (17)$$

$$n = 22, \quad r = 0.8950, \quad sd = 0.174, \quad F = 24.1$$

Here and elsewhere, n is the number of data points, r is the correlation coefficient, sd is the standard deviation, and F is the F-statistic. The characterisation of gas-solid adsorption is harder to study than is gas-liquid absorption, due to the non-homogeneous surface of the solid. In addition, the range of adsorbate concentration that allows linearity of isotherm is very much smaller than in gas-liquid systems.

The regression equation for C_{60} reveals that it is quite basic, with a = 1.04, thus showing selectivity towards hydrogen-bond acid solutes. The hydrogen bond basicity of C_{60} is no doubt due to the high electron density around the ball. The regression equation also suggests that it is fairly polar, s = 0.72, although this value is perhaps lower than expected from its type of structure. Taylor and Walton [11] however, have suggested that fullerenes do not behave as highly aromatic molecules, but as giant closed-cage alkenes. The s-constant in eq(16) is certainly compatible with this suggestion. The dispersion interaction term in eq(16) is rather small, l = 0.47, and so the selectivity in terms of solute size does not play a such a major role as with other adsorbents.[12] The r coefficient gave a small negative value, r = -0.237, when an interaction between n and π electrons is expected to be fairly dominant. A possible explanation could be due to the repulsion between the electrons in the fullerene 60 and the solute lone pairs. Note that the $b.\Sigma\beta^H_2$ term is dropped in the regression eq(16), due to a very poor significance test. This means that hydrogen bond bases are inactive towards C_{60}, or, conversely, that C_{60} has no hydrogen bond acidity.

Overall, the result yields some insight into the many possible properties of this highly stable new form of carbon. This is the first time that C_{60} has been examined as a potential adsorbent and shows that there is possible use of the fullerene as a selective adsorbent.

3.6 Graphite

In order to have a standard adsorbent with which to compare our previous results, we selected graphite. The solid phase studied was in the form of graphite flakes obtained from Aldwych and dried in a vacuum dessicator. The required mesh size 20-30 was obtained by sieving the solid, which was packed into a short

column (0.2388g) and conditioned in helium for 24 hours at 200°C. A standard solute was chosen which did not have a very long retention time, so that it could be injected from time to time, especially after the column was reconditioned. This served as a check that the surface of the graphite was the same ie. that reproducible results could be obtained.

The same set of solutes as for the fullerenes was used to probe the interaction character of graphite. Results for 22 adsorbates were obtained using our general data analysis programme to calculate the gas-solid partition coefficient. This was calculated as K_c and K_p; values are in Table 1. Application of the general solvation equation to the $\log K_c$ and $\log K_p$ values leads to the following equations:

$$\log K_c = -1.548 - 0.259\ R_2 + 0.989\ \pi^H_2 + 1.106\ \Sigma\alpha^H_2 + 0.587\ \log L^{16} \quad (18)$$

n = 22, r = 0.9712, sd = 0.117, F = 70.6

$$\log K_p = -1.192 + 0.831\ \pi^H_2 + 0.772\ \Sigma\alpha_2^H + 0.679\ \log L^{16} \quad (19)$$

n = 22, r = 0.9536, sd = 0.143, F = 60.0

The regression results obtained are quite good, with reasonable correlation coefficients and standard deviations. The dispersive interaction does not play a dominant role, but this is as expected for a carboneous phase, l = 0.587 for $\log K_c$ and l = 0.679 for $\log K_p$. Graphite has a negative coefficient for r, r = -0.259 for $\log K_c$, and r is insignificant for $\log K_p$. This indicates that there is no interaction via n-π electrons, but possibly that some lone pair-lone pair electron repulsion occurs. A distinguishing feature of the correlation equations is the term in solute hydrogen-bond acidity, indicating interactions via hydrogen-bond basic sites in graphite, a = 1.106 for $\log K_c$ and a = 0.772 for $\log K_p$. These values are rather high for a phase that has only π-electron functions as electron donor sites; note that the graphite structure consists of sheets of fused benzene rings stacked together. As expected of a structure of fused benzene rings, graphite is dipolar/polarizable: s = 0.989 for $\log K_c$ and s = 0.831 for $\log K_p$. The absence of hydrogen bond acidity agrees with the nature of graphite, since no electron acceptor function exists. Results of the correlations for adsorption on graphite and fullerenes are remarkably similar, and confirm our above conclusions on the chemical nature of fullerene. As well as studying the 22 solute data set for comparison with fullerene, we examined the more extensive data set in Table 1,

$$\log K_c = -0.856 - 0.273\ R_2 + 0.864\ \pi^H_2 + 0.939\ \Sigma\alpha^H_2 + 0.458\ \log L^{16} \quad (20)$$

n = 36, r = 0.9700, sd = 0.148, F = 123.6

$$\log K_p = -0.616 + 0.726\ \pi^H_2 + 0.628\ \Sigma\alpha_2^H + 0.570\ \log L^{16} \quad (21)$$

n = 36, r = 0.9781, sd = 0.144, F = 235.7

The equations for the extended data set are well in line with those for the 22 solute data set, above, and the general conclusions as to the nature of graphite remain unchanged. However, we prefer eq(20) and eq(21) as the best set of equations for the characterisation of graphite.

Table 1. Fullerene and Graphite $\log K_c$ and $\log K_p$ at 298K

	graphite		fullerene	
Solute	$\log K_c$	$\log K_p$	$\log K_c$	$\log K_p$
Decane	1.14	1.91	0.55	1.310
Undecane	1.53	2.33	0.85	1.650
Dodecane	1.82	2.66	1.21	2.050
1,1,2,2-tetrachloroethane	1.33	2.16	0.96	1.800
Tetrachloroethene	0.83	1.66	0.57	1.410
Methylene iodide	1.20	2.24	0.54	1.580
Butylether	1.11	1.83	0.54	1.270
Octan-2-one	1.50	2.22	0.93	1.650
Decan-2-one	2.19	2.99	1.51	2.320
Butyl propanoate	1.21	1.94	0.54	1.260
Octan-1-ol	2.17	2.89	1.22	1.950
Dimethylsulphoxide	2.17	2.67	1.16	1.670
Triethylphosphate	2.13	3.00	1.49	2.360
Propylbenzene	1.13	1.82	0.49	1.180
1,2-Dichlorobenzene	1.55	2.33	0.82	1.740
4-Chlorotoluene	1.48	2.19	0.52	1.730
Iodobenzene	1.53	2.45	0.89	1.750
Nitrobenzene	2.13	2.83	1.17	1.890
m-Cresol	2.13	2.78	1.51	2.150
2-Chlorophenol	1.81	2.52	1.24	1.960
Benzyl alcohol	2.12	2.76	1.20	1.850
Pyrrole	1.14	1.57	0.53	1.000
Hexane	0.36	0.91		
Norbornane	0.73	1.32		
Decalin	1.77	2.53		
a(+-)-Pinene	1.05	1.80		
Norbornylene	1.05	1.64		
Dichloromethane	0.35	0.90		
Tetrachloromethane	0.65	1.45		
Tetrahydrofuran	0.71	1.18		
Propanone	0.76	1.14		
Norcamphor	1.74	2.39		
Methanol	0.35	0.47		
Benzene	0.75	1.25		
Toluene	1.05	1.63		

3.7 XAD-16

This solid is a polyvinylbenzene nonionic resin, of general structural formula,

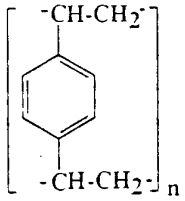

Figure 1

The solid was sieved to a 20-30 mesh size, and packed into two columns with wider bore to minimise the presure drop across the column. One was a short column (length = 3.5cm, width = 3.0mm and post-conditioned weight = 0.0573g), and the other was a longer (length = 10.5cm, width = 3.0mm and post-conditioned weight = 0.1527g); this was to reduce the retention times on larger size solutes. Care was taken to check the consisitency of the K-values on the two columns. The packed columns were conditioned under steady flow of helium gas at 323K for 24 hours, as higher temperature slightly melted some of the solid pellets. The flow rate of the carrier gas was chosen to yield minimum plate height equivalent; a flow rate of 40 ml/min was selected. The column temperature was maintained at 298K by means of a water thermostat into which the column was placed. Data were collected and processed as described above. Results are in Table 2. Application of eq(1) to data for 23 solutes gave the equations,

$$\log K_c = -0.895 - 0.923\ R_2 + 0.252\ \pi^H_2 + 1.179\ \Sigma\alpha^H_2 + 0.897\ \Sigma\beta^H_2 + 1.304\ \log L^{16} \qquad (22)$$

$n = 23, \quad r = 0.9704, \quad sd = 0.178, \quad F = 54.9$

$$\log K_p = -0.624 - 1.334\ R_2 + 0.580\ \pi^H_2 + 1.318\ \Sigma\alpha^H_2 + 0.404\ \Sigma\beta^H_2 + 1.450\ \log L^{16} \qquad (23)$$

$n = 23, \quad r = 0.9704, \quad sd = 0.178, \quad F = 54.9$

This polymeric solid shows a rather strong dispersive interaction with solutes, and this the reason why it was difficult to study larger sized solutes. For example hexane took 17 hours to 'completely' elute from the column, and each solute had to be chromatogrammed several times in order to obtain reliable results. XAD-16 shows quite strong hydrogen bond interactions, as indicated by a significant a-constant (1.387) and a significant b-constant (0.931). Although the a-constant, due to the solid phase basicity is as expected, this is not so for the b-constant. there is no structural feature in Figure 1 to suggest any solid phase acidity. The solid was therefore examined with an electron microprobe, and the presence of a small amount of oxygen atoms was detected. This result was partly confirmed by use of Fast

Atom Bombardment (FAB) mass spectroscopy, which showed a very small peak at m/z = 413, that we think is due to the presence of plasticiser in the solid. Examination by Electronic Ionisation (EI) mass spectrometry showed a peak at m/z = 149 that is also due to the presence of plasticiser, plus an intense peak at m/z = 18 due to water. Solid state NMR identified the divinylbenzene polymeric structue, but no chemical shift due to oxygen was observed; this is not surprising because of the comparitively low sensitivity of solid state NMR. The FTIR spectrum of XAD-16 showed the presence of OH as a small broad band at 3600 cm^{-1} even though the solid was dried over P_2O_5 in vacuo. Interestingly, two small peaks were observed at 1750 and 1100 cm^{-1} corresponding to C=O and C-O respectively. It is very likely that these peaks are due to plasticiser.

Our conclusion is that the solid XAD-16 is contaminated with plasticiser that contains C=O and C-O bonds and which forms active sites on the surface. This is why the solvation equation contains terms in solute acidity, eq(22) and eq(23). This analysis suggests that the presence of quite small impurities in a solid can markedly affect sorption properties, and also that the solvation equation approach is sensitive enough to detect this.

3.8 XAD-7

This adsorbent, XAD-7, is a poly(methacrylic ester) resin with the general structural formula below, and was studied at 298K.

$$\left[\begin{array}{l}\text{-CH-} \\ \text{COOR}\end{array}\right]_n$$

The adsorbent was first sieved to a mesh size of 20-30, and the white solid was then packed into a column 7 cm in length, and a width of 3.0mm. The packed column was conditioned under a steady flow of helium (55ml/min) at 340K for 24 hours. This process of conditioning was necessary to rid the porous surface of the adsorbent of any contaminants, such as moisture. The weight of solid adsorbent reduced after conditioning from 0.2104g to 0.1977g . This small loss in weight is considered to be due to loss of moisture at the temperature the solid was conditioned. The weight of the adsorbent, 0.1977g, and the carrier gas flow, 55 ml/min, were selected such that the adsorption between the gaseous solute and the polymeric solid was in equilibrium, and the elution time was not too long. The above selection was carried out by first testing a few hydrocarbons as solutes. Two standard solutes were then selected for this adsorbent, butane and pentane. Butane was used as a standard very frequently to check that the adsorbent surface was cleared of the previous gaseous solute as much as possible, by ensuring that the elution time was reproducible. Pentane has a much longer elution time (8 hours) so it would give a much better idea of the state of the surface. Both butane and pentane were used as standards after the column was reconditioned, as a check that the adsorbent surface was consistent. It is important that the solid be conditioned as

often as possible at 420K to rid the surface of any remains of strongly retained solutes.

XAD-7 is a very strong polymeric adsorbent, depending on the solute size and adsorbate, but most of the probes took very long times to elute, some as long as 40 hours. In order to obtain reproducible results all the probes were run at least twice. The data were collected via a personal computer on an Unkelscope software, and by using a data analysis programme, the gas-solid partition coefficient, K, was calculated as $\log K_c$ and $\log K_p$, defined by eq(5) and eq(6).

The set of probes used in this work is set out in Table 2, together with the obtained values of $\log K_c$ and $\log K_p$, and those obtained by McGill.[13] Results are similar to those of McGill except for very long retained solutes. Aplication of the general solvation equation (1) leads to the following:

$$\log K_c = -0.321 - 1.401\ R_2 + 1.11\ \pi^H_2 + 1.29\ \Sigma\alpha^H_2 + 0.525\ \Sigma\beta^H_2 + 1.07\ \log L^{16} \quad (24)$$

$n = 22, \quad r = 0.9695, \quad sd = 0.141, \quad F = 50.0$

$$\log K_p = -0.047 - 1.779\ R_2 + 1.442\ \pi^H_2 + 1.45\ \Sigma\alpha^H_2 + 1.215\ \log L^{16} \quad (25)$$

$n = 22, \quad r = 0.9579, \quad sd = 0.174, \quad F = 47.4$

The equations obtained show, as expected, that this adsorbent has a quite strong hydrogen-bond basicity interaction, (a=1.29 for $\log K_c$ and a=1.45 for $\log K_p$) due to the presence of the ester group, see Figure 1. This of course also means that the phase is fairly polar, (s=1.110 for $\log K_c$, s=1.442 for $\log K_p$). There is present also a small amount of hydrogen-bond acidity, (b=0.525 for $\log K_c$, but statistically insignicant for $\log K_p$ at 95% t-test), possibly due to the acidic proton alpha to the ester group. The dispersive interaction is fairly dominant, (l=1.071 for $\log K_c$ and l=1.215 for $\log K_p$) as is mostly the case for adsorption.

The results obtained for $\log K_c$ and $\log K_p$ by McGill on XAD-7, see Table 2, were regressed against our current solute parameters so that the solutes descriptors used are the same for both McGill's results and the present results, enabling comparison to be made.

$$\log K_c = -0.881 - 0.316\ R_2 + 0.673\ \pi^H_2 + 0.918\ \Sigma\alpha^H_2 + 0.675\ \Sigma\beta^H_2 + 0.775\ \log L^{16} \quad (26)$$

$n = 19, \quad r = 0.8714, \quad sd = 0.263, \quad F = 8.2$

$$\log K_p = -1.073 - 0.646\ R_2 + 0.356\ \pi^H_2 + 0.786\ \Sigma\alpha^H_2 + 1.134\ \Sigma\beta^H_2 + 1.076\ \log L^{16} \quad (27)$$

n = 19, r = 0.9041, sd = 0.307, F = 11.6

The two sets of equations thus obtained agree quite well within experimental error, except for the intercept. This is because the values obtained by McGill are systematically smaller by nearly one log unit. McGill used a Thermal Conductivity Detector (TCD) to carry out his studies, and the TCD sensitivity is much lower than that of a FID detector. This means that the observed elution time of a solute will always be much smaller using a TCD detector than that observed with a FID detector, and leads to the calculated values of $\log K_c$ and $\log K_p$ always being less in the TCD than the FID method.

Table 2. XAD-7 and XAD-16 $\log K_c$ and $\log K_p$ at 298K

Solute	XAD-16 $\log K_c$	XAD-16 $\log K_p$	XAD-7 $\log K_c$	XAD-7 $\log K_p$	$\log K_c$ McGill's	$\log K_p$ McGill's
Butane	1.33	1.71	1.24	1.62	0.30	0.68
Pentane	1.89	2.36	2.23	2.69	0.98	1.45
Hexane	2.59	3.20	2.53	3.14	1.14	1.68
Heptane	-	-	-	-	1.61	2.23
Cyclohexane	2.79	3.33	2.48	3.02	-	-
Methylene chloride	1.60	2.14	1.90	2.44	1.63	1.09
Chloroform	2.30	2.99	2.51	3.20	1.40	2.08
Tetrachloromethane	2.33	3.13	2.62	3.42	1.09	1.89
Freon 21	-	-	1.50	2.13	-	-
Freon 12	0.49	1.18	0.94	1.64	-	-
Diethylether	1.93	2.43	2.26	2.74	0.98	1.46
Acetone	-	-	2.55	2.94	1.41	1.78
Butanone	2.59	3.06	2.94	3.40	1.51	1.98
Methylformate	0.90	1.27	1.63	2.02	-	-
Methylacetate	2.34	2.82	2.55	3.03	-	-
Ethylacetate	2.56	3.11	2.79	3.35	1.40	1.96
Ethylamine	1.97	2.23	-	-	-	-
Propylamine	2.87	3.26	2.53	2.92	-	-
Water	-	-	-	-	0.41	0.27
Methanol	1.21	1.33	1.65	1.77	0.46	0.27
Ethanol	1.60	1.90	2.25	2.55	1.26	1.54
Propanol	2.32	2.71	2.55	2.94	1.80	2.19
Propan-2-ol	-	-	2.53	2.92	1.59	1.98
t-Butanol	2.33	2.81	2.44	2.98	1.57	2.05
TFE	1.96	2.57	2.51	3.12	-	-
Benzene	2.51	3.01	2.44	2.95	1.46	2.00
Toluene	-	-	-	-	1.83	1.95

3.9 Chromosorb GAW-DMCS

To gain an insight into any possible adsorption effects of the inert support used in the gas-liquid chromatographic work, a study was made using Chromosorb GAW-DMCS as a solid adsorbent. This Chromosorb is the one used in all the GLC work described in this report. A column of the Chromosorb of length 1.45m, width 3.0mm, and of weight 6.3614g was packed and conditioned as usual, and measurements of relative and absolute retention volumes were carried out. The reason why retention volumes were measured, and not gas-solid adsorption coefficients, is that any correction in GLC from adsorption on the solid suport requires V_G data. For 22 varied solutes at 298K, $\log V_G$ values were obtained as shown in Table 3. Application of eq(1) yielded,

$$\log V_G = - 2.43 - 0.30\ R_2 + 0.35\ \pi^H_2 + 2.13\ \Sigma\alpha^H_2 + 2.05\ \Sigma\beta^H_2 + 0.69\ \log L^{16} \qquad (28)$$

$$n = 22, \quad r = 0.9650, \quad sd = 0.144, \quad F = 43.3$$

It was difficult to obtain exactly the same set of solutes as in the GLC work with polymeric phases, due to the long retention time, and considerable peak tailing of solutes. A number of solutes failed to elute at all; these included dimethyl sulfoxide, dimethylformamide and triethylamine. From the regression equation, the largest coefficients are a = 2.13, b = 2.05, and l = 0.69 , so that the support is basic, and acidic, as well as retaining solutes by general dispersion interactions. The acidity and basicity shown by the support is rather unexpected, because the support is silanised and acid-washed to remove any acidic and basic sites.[9] However, this treatment only minimises the activity of the hydrogen bond interactions, and does not reduce them altogether. The large hydrogen bond interactions may be the cause of very evident tailing of alcohols and various basic solutes when characterising columns containing only small percentages of stationary phase.

3.10 Conclusions on the IGC of Adsorbents

Our experimental set-up with the FID detector is a very powerful method for obtaining the data required to characterizs adsorbents through the solvation equation. Under the experimental conditions, adsorption is examined at very low surface coverage of the adsorbent, so that the presence of rather small numbers of active sites on the adsorbent can exert considerable effects on the solvation equation. This seems to be the case for XAD-17, that showed considerably more hydrogen-bond acidity and basicity than expected from its structure. We examined this adsorbent in more detail than the others, and were able to show by a number of methods, that the adsorbent contained oxygen atoms, probably as C-O and C=O bonds, and perhaps also as O-H bonds. In our view it seems essential to examine samples of adsorbents by the various mass spectrometry and FTIR methods, see above, in order to detect possible contaminating species.

The analysis using the solvation equation is sensitive enough to respond to the presence of small quantities of contaminant. No doubt at low surface coverage these contaminants can provide active sites on the surface that have an effect on adsorption far beyond their stoichiometric quantity.

A summary of the equations for the adorbents is in Table 4.

Table 3. Inert Support GAW(DMCS) 40-60 Mesh at 298K

Comp. name	$logt_{rel}$	$logV_G$
Octane	0.000	0.012*
Nonane	0.485	0.494
Decane	0.973	0.834*
Undecane	1.376	1.385
Methylene Iodide	0.497	0.506
Butyl ether	0.751	0.864*
Tetrahydrofuran	0.809	0.818
Pentan-2-one	0.772	0.781
Heptan-2-one	1.427	1.395*
Pentyl acetate	1.303	1.312
Butyl-propionate	1.253	1.279*
Ethanol	0.530	0.539
Propanol	0.955	0.991*
Butanol	1.383	1.392
Hexafluoroisopropanol	0.568	0.577
Propylbenzene	0.626	0.605*
Butylbenzene	1.207	1.015*
Chlorobenzene	0.285	0.282*
1,2-Dichlorobenzene	0.936	1.013*
4-Chlorotoluene	0.608	0.664*
Iodobenzene	0.950	0.959
Phenol	2.247	2.256

* The $logV_G$ values used as standards.

Table 4. Inverse Gas-chromatography of Adsorbents at 298K

Phases	c	r	s	a	b	l	n	R	sd	F
Fullerene (C_{60},C_{70}),										
$\log K_c$-	1.580	-0.237	0.721	1.041	-	0.477	22	0.9506	0.124	39.8
$\log K_p$	-1.093	-	0.576	0.596	-	0.549	22	0.8950	0.174	24.1
Graphite										
$\log K_c$	-1.548	-0.259	0.989	1.106	-	0.587	22	0.9712	0.117	66.1
$\log K_p$	-1.192	-	0.831	0.772	-	0.625	22	0.9536	0.143	60.0
$\log K_c$	-0.856	0.273	0.864	0.939	0.458	0.460	36	0.9700	0.148	123.6
$\log K_p$	-0.616	-	0.726	0.628	-	0.570	36	0.9781	0.144	235.6
Poly(divinylbenzene)										
$\log K_c$	-0.895	-0.932	0.252	1.179	0.897	1.304	23	0.9700	0.178	54.9
$\log K_p$	-0.624	-1.334	0.580	1.318	0.404	1.450	23	0.9700	0.195	54.1
Poly(methacrylic ester)										
$\log K_c$	-0.321	-1.401	1.110	1.290	0.525	1.071	22	0.9695	0.141	50.0
$\log K_p$	-0.047	-1.779	1.442	1.450	-	1.215	22	0.9579	0.174	47.4

4. Gas-liquid Chromatography

The use of inverse gas chromatography to characterise polymeric stationary phases is now a well-known method. In brief, the method consists of the determination of specific retention volumes, V_G, at the column temperature, 298K, for a set of solutes, followed by an analysis of the data by a multiple linear regression method. We consider the results obtained using the Linear Solvation Energy Relationship (LSER) generated from the multiple linear regression analysis. Since GLC is a well understood technique, we set out only the elements of GLC, together with the equations we shall use.

4.1 Retention time and volume

Sample molecules spend part of their time in the mobile phase, as well as the stationary phase, during their passage through the chromatographic column. All molecules spend the same amount of time in the mobile phase refered to as the column dead time or hold up time, t_m , equivalent to the time required for an unretained solute to reach the detector from the point of injection. The retention time of a solute ,t_r, is the time the average molecule of solute takes to travel the whole length of a chromatographic column and is measured to the midpoint of the elution curve. The measured t_r includes the time ,t_m, taken by the solute to pass through the carrier gas from the column inlet to outlet. The retention volumes V_r and V_m are obtained when t_r and t_m are respectively multiplied by the gas flow rate ,F, at the column outlet presure. Under a given set of operating conditions F is a constant and therefore t_r can be used in place of V_r . The true retention time, t_r', or retention volume ,V_r', of the solute is found by subtracting t_m from t_r or V_m from V_r as appropriate. Within a homologous series , retention time increases with increasing molecular weight. In GLC the retention volume has to be corrected for the compresibility of the gaseous mobile phase due to the pressure differential along the column. Thus, as the measurements of retention times are made at the outlet pressure there is the need to correct to mean column pressure. To do this , the pressure gradient correction term ,J, in eqn(14) is introduced. As a consequence, the net retention volume ,V_n, which can be used to calculate equilibrium thermodynamic parameters such as the activity coefficient can be calculated as follows, where the corrected flow rate is defined as in eq(15):

$$V_r' = V_r - V_m = F(t_r - t_m) \quad (29)$$

$$t_r' = t_r - t_m \quad (30)$$

$$V_n = JFt_r' = JV_r' \quad (31)$$

The quantities V_r and V_m or t_r and t_m include any extracolumn dead spaces which are swept by the gas between the centres of the detector and the injector . Nevertheless, these dead spaces do not contribute to V_n because they cancel out when V_m is subtracted from V_r or t_m is subtracted from t_r. In practice, the net retention time is usually obtained by measuring the distance

t_r on the recorder chart between the peak of a non-sorbed solute and that of the sorbed solute. As the flow rate is determined with a soap film meter it is necessary to correct this value for both the vapour pressure of the soap solution which is assumed to be equal to the vapour pressure P_w of pure water at the meter temperature and also for the difference between the column and flow meter temperature. The gas hold up volume ,V_m, or time ,t_m, retention is commonly determined by the air peak or inert gas peak method which merely requires injecting a sample of air or other non sorbed gas whose retention volume is taken as the gas hold up. The choice of a non sorbed gas depends partly on the detector and the carrier gas, as the carrier gas is chosen to maximise the detector response. In the case of a Katharometer any gas which has a thermal conductivity different from the carrier gas can be used. Thus, for hydrogen or helium as carrier gas it is convenient to include a small volume of air with the sorbed solute. However, a flame ionisation detector (FID) does not normally respond to inorganic materials making it necessary to use methane for the inert gas peak for GLC work.

4.2 Relative retention time and specific retention volume

The relative retention time is defined by the ratio of adjusted retention time of a solute and a standard determined under identical conditions. The specific retention volume ,V_G, is the net retention volume per unit mass of the stationary phase at the column temperature. V_G^o is the specific retention volume corrected to 273K. V_G is related to the partition coefficient L, [defined in eq(33)] by the equation:

$$L = \rho \cdot V_G \qquad (32)$$

where ρ is the density of the stationary phase at the column temperature. Note that in the calculation of thermodynamic quantities, V_G at the column temperature must be used.

L = [conc of solute in solution]/[conc of solute in the gas] (33)

The relative retention time is obtained from the chromatogram as follows:

$$trel = (t_r2 - t_m)/ (t_r1 - t_m) \qquad (34)$$

where trel is the relative retention time and t_r2 ,t_r1 and t_m are the retention times of solute, standard and air peak respectively. Usually, an n-alkane is chosen as the standard as alkanes are readily available in the pure form. The use of relative retention times has the advantage that effects of slight variation of column temperature, injection technique,and stationary phase loading are minimised because the retentions of both standard and solute are affected to the same extent.

4.3 Butyl rubbers

A number of butyl rubbers of general formula,

$$-(CH_2-CH_2CH[CH_3])_n-$$

were examined in the usual way. The rubbers were denoted as 388P, B178, and B174. They were opaque, rubbery and soluble in toluene.

In all cases, only low % loadings, <5%, on the inert support could be obtained. The $\log V_G$ values for a series of solutes on these phases at 298K were obtained as described above. Considerable peak tailing was observed, no doubt party due to the low % loadings. Hence the results from the MLRA analysis will not be as clear cut as usual, because of the possibility of adsorption on the inert support.

4.3.1 Butyl rubber 388P

Butyl rubber was coated on chromosorb GAW-DMCS 40-60 mesh size at 5.5847% loading. The coated support after the solvent had evaporated off at room temperature was packed into two columns. The longer column had a length of 95cm, bore of 3.0mm and a packing weight of 4.0725g. This column was used on small size molecules which have low retention times and was the main column used. The shorter column had a packed length of 42.5cm, a bore of 3.0mm and contained 1.8803g of coated support. Values of $\log V_G$ were obtained for 42 solutes, Table 5, and application of the general solvation equation yielded,

$$\log V_G = -0.932 + 0.226\ R_2 + 0.261\ \Sigma\alpha^H_2 + 0.349\ \Sigma\beta^H_2 + 1.102\ \log L^{16} \quad (35)$$

$n = 42, \quad r = 0.9961, \quad sd = 0.068, \quad F = 1187.0$

The rubber has no dipolarity/polarizability, and only a little hydrogen-bond basicity and acidity. The l-constant is very large, so that 388P interacts with solutes mainly through general dispersion effects.

4.3.2 Butyl rubber B178

Exactly the same procedure of coating was carried out on B178, with a percentage loading of 5.4276%. Again two columns were packed, a longer column (length = 97.8cm, bore = 2.0mm and weight = 2.1985g), and a shorter column (length = 42.5cm, bore = 2.00mm and weight = 0.9626g). The resultant $\log V_G$ values led to the following regression,

$$\log V_G = -1.276 + 0.260\ R_2 + 0.326\ \Sigma\alpha^H_2 + 0.415\ \Sigma\beta^H_2 + 1.146\ \log L^{16} \quad (36)$$

$n = 42, \quad r = 0.9956, \quad sd = 0.074, \quad F = 1050.7$

Again, the rubber exhibits little hydrogen-bond basicity or acidity, but gives rise to a large l-constant. Hence the main interaction with solutes will be by dispertion interactions.

Table 5. Butyl Rubber $logV_G$ at 298K

Comp. name	B178 $logV_G$	388P $logV_G$	B174 $logV_G$
Heptane	2.303	2.624	2.478
Octane	2.911*	3.197*	2.972*
Nonane	3.543*	3.211	3.606*
Decane	4.055	4.335	4.170
1,1,2,2-Tetrachloroethane	3.340	3.620	3.409
1-Chlorobutane	1.939	2.276	2.045
Trichlorethylene	2.399	2.661*	2.447
Tetrachloroethene	3.058*	3.318*	3.133*
Methylene iodide	3.700	3.823	3.649
Di-n-Butylether	3.272*	3.568	3.382*
Tetrahydrofuran	1.939	2.229	1.947
1,4-dioxane	2.397	2.169	2.536
Pentan-2-one	2.095	2.548*	2.412
Heptan-2-one	3.298	2.355*	3.484*
Octan-2-one	3.920	3.541	3.911
Nonan-2-one	4.387	4.064	4.449
Propyl formate	1.665	4.571	1.907
Butyl propanoate	3.383	1.785	3.474
Formamide	2.979	3.564	3.076
Dimethylformamide	2.918	2.974*	3.640
N,N-Dimethyacetamide	3.450	3.597	2.891
Pentanol	2.763	2.865*	3.299
Hexanol	3.365*	3.413*	3.953
Heptanol	3.840	3.934	4.372
Octanol	4.306	4.536	3.639
Dimethysulfoxide	2.979	3.538	4.474
Triethylphosphate	4.649	4.747	2.804
Toluene	2.741	2.968	3.301*
Ethylbenzene	3.207*	3.456*	3.479
o-Xylene	3.466	3.663	3.777*
Propylbenzene	3.710*	4.023	4.382
Butylbenzene	4.398	4.479	3.133*
Chlorobenzene	3.139*	3.360*	4.182
1,2-dichlorobenzene	4.153	4.312	3.805
4-chlorotoluene	3.838	3.971	4.277
Iodobenzene	4.181	4.330	3.949
Aniline	3.710*	3.885	3.726*
Phenol	3.571*	3.874	4.300
m-Cresol	4.122	4.338	3.983
2-Chlorophenol	4.018	4.000	4.248
Benzyl alcohol	4.068	4.260	3.997
3-Ethylpyridine	3.837	4.012	2.470
Pyrrole	2.372	2.548*	2.598

* $LogV_G$ values used as standards.

4.3.3 Butyl rubber B174

The last butyl rubber was coated at 5.0942%. The resultant coated support was packed into two columns, a longer column (length = 97.0cm, bore = 2.0mm and weight = 2.1404g), and a shorter column (length = 40.5cm, bore = 2.0mm and weight = 0.9158g). Regression of $\log V_G$ for the 42 solutes yields,

$$\log V_G = - 0.932 + 0.283\ R_2 + 0.333\ \Sigma\alpha^H_2 + 0.557\ \Sigma\beta^H_2 + 1.076\ \log L^{16} \qquad (37)$$

n = 42, r = 0.9917, sd = 0.098, F = 548.7

The regression equation is not so good as for the previous two rubbers, but still shows the same features; the predominant interaction with the studied solutes is through general dispersion interactions.

All three butyl rubbers have little dipolarity, acidity, or basicity, and hence will appear inert to corrosive or reactive chemicals by processes of sorption. Of the three polymers, 388P has less hydrogen-bond basicity than the other two.

4.4 Epom Duponts 'Nordel' hydrocarbon (Epom polymer)

This is a synthetic rubber of ethylene-propylene-hexadiene hydrocarbon. It is light-amber and comes in the form of rather tough pellets, it could be dissolved in cyclohexane by refluxing for several hours. The polymer could be coated onto the inert support (GAW-DMCS, 40-60 mesh size) only to about 4% loading. The exact percentage loading was found by ashing the coated support to a constant weight. The resultant coated support was packed into a Pye Unicam 104 Series glass column, and then conditioned under a steady flow of dried helium gas over night. For the retention volume determinations a carrier gas (helium) flow rate was chosen to give a minimum plate height equivalent, and was 35ml/min. Data on 41 solutes were collected, and are given in Table 6 as values of $\log V_G$. Application of eq(1) to these values yielded,

$$\log V_G = - 0.154 + 0.204\ R_2 + 0.389\ \Sigma\alpha^H_2 + 0.206\ \Sigma\beta^H_2 + 0.943 \log L16 \qquad (38)$$

n = 42, r = 0.9950, sd = 0.063, F = 931.1

The above equation shows that Epom polymer is rather inert, and interacts with solutes mainly according to their size, as shown by the l-constant (l= 0.943). There are small effects of the R_2 descriptor and the dipolarity/polarizability term (s=0.194). Epom polymer contains only hydrocarbon, and is not therefore expected to have any acidic or basic properties. However, the hydrogen-bond basicity of the polymer (a= 0.429) is small but significant. This may be due to a slightly basic carbon as a result of inductive effect across the polymer chain, or could be due impurities in the polymer.

Table 6. Epom 'Nordel' Hydrocarbon Polymer at 298K

Compound name	$logt_{rel}$	$logV_G$	
Heptane	-0.471	2.826	
Octane	0.000	3.297	*
Nonane	0.488	3.777	*
Decane	0.969	4.266	
1,1,2,2tetrachloroethane	0.331	3.628	
1-Chlorobutane	-0.838	2.459	
Trichloroethylene	-0.514	2.740	*
Tetrachloroethene	0.069	3.366	
Iodoemethane	0.470	3.767	
Butyl ether	0.266	3.592	*
Tetrahydrofuran	-0.807	2.490	
1,4-Dioxane	-0.522	2.775	
Pent-2-one	-0.815	2.482	
Heptan-2-one	0.190	3.483	*
Octan-2-one	0.661	3.958	
Cyclohexanone	0.160	3.457	
Propyl formate	-1.091	2.206	
Pentyl acetate	0.067	3.364	
Butyl propanoate	0.240	3.566	*
Triethylamine	-0.174	3.123	
Dimethylformamide	-0.098	3.199	
Pentanol	-0.203	3.094	
Hexanol	0.284	3.529	*
Heptanol	0.734	4.031	
Octanol	1.088	4.385	
Cyclohexanol	0.363	3.660	
Dimethylsulphoxide	0.515	3.812	
Triethyl phosphate	1.237	4.534	
Toluene	-0.158	3.139	
Ethylbenzene	0.219	3.534	*
o-Xylene	0.420	3.717	
Propylbenzene	0.660	3.943	*
Butylbenzene	1.114	4.411	
Chlorobenzene	0.132	3.429	
1,2-Dichlorobenzene	0.984	4.281	
4-Chlorotoluene	0.678	3.975	
Iodobenzene	1.053	4.350	
Aniline	0.601	3.898	
Phenol	0.640	3.949	*
m-Cresol	1.027	4.324	
o-Chlorophenol	0.761	4.058	
Benzyl alcohol	0.962	4.259	
3-Ethylpyridine	0.646	3.943	
Pyrrole	-0.573	2.724	

* Used as standards.

Another possibility that may explain the slight basicity of the polymer is the interaction of the probes with the inert support, since the polymer coating was low (3.966%). This is further supported by the tailing of peaks for most of the solutes, especially alcohols. In any event, it is unlikely that the small basicity result is caused by the presence of moisture in the polymer, because of the constant flow of dried carrier gas.

4.5 Poly(vinylidene fluoride-co-hexafluoropropylene) (Fluorel FC-2174)

Fluorel FC-2174 is reported as containing 95-98% copolymer of 1,1-difluoroethene and 1,1,2,3,3,3-hexafluoropropylene, and 2-3% of other compounds; phenol,4,4'[2,2,2-trifluoro-1-(trifluoro -methyl)ethylidene]bis...benzene,1,1'-sulfonylbis[4-chloro-.....

The copolymer has a general structural formula:

$$(-CH_2-CF_2-)_n(-CF_2-CF[CF_3]-)_m$$

This Fluorel co-polymer has a creamy colour in appearance, and it is fairly rubbery. It is soluble in the solvent 1,1,3-trichlorotrifluoroethane at room temperature, and was coated onto Chromosorb GAW-DMCS of (40-60) mesh size at a 12.442% loading. The solvent was allowed to evaporate off slowly at room temperature with occasional gentle stirring. After all the THF had vaporised, the Fluorel polymer coated onto the support was dried in a vacumn dessicator containing phosphorous pentoxide (P_2O_5). The end product was a smooth homogeneous coated support. This coated support was packed into a column of length 95cm and width of 3.0mm, and weighed 4.5164g; it was conditioned in dried helium at 301K over the weekend. A higher temperature was not used, because this Fluorel polymer might be thermally unstable. A carrier gas flow rate that would give a good column efficiency was selected, (30ml/min), and a hydrocarbon, nonane, was chosen as a reference solute. Nonane like most alkanes is a good standard, because of its purity and is symmetrical in peak shape, with no tailing. A set of probes with wide ranging parameters in which the correlation between the parameters was low, were selected , and their $\log V_G$ values obtained in the usual way, see Table 7. Application of the general solvation equation and regression analysis resulted in the following equation:

$$\log V_G = -0.937 - 0.275R_2 + 1.828\ \pi^H_2 + 2.365\ \Sigma\alpha^H_2 + 1.114\ \Sigma\beta^H_2 + 0.779\ \log L^{16} \qquad (39)$$

$n = 34, \quad r = 0.9948, \quad sd = 0.078, \quad F = 536.5$

This Fluorel polymer generally interacts quite strongly with many of the solutes used, some taking as long as 7 hours to elute. Some of the larger molecules, such as phenol, chlorophenol and pyridine could not be eluted at all. Almost all solutes had symmetrical peaks with no observable tail; this is due to the high percentage loading on the support. However, there was slight column bleeding as time went on, and this was shown up by the change in the retention of the standard, and the downward slope

change in the retention of the standard, and the downward slope of the baseline of the FID detector. The exact weight of the polymer on the column had to be found by destroying the column at the end of the experiments, and ashing the packing to a constant weight using a Bunsen burner. The ashing of this sample took 5 days at ~1100K before all the polymer was burnt off, and so the slight bleeding on the column was rather surprising. To ensure that the small loss of stationary phase makes little or no difference to the $\log V_G$ values, another set of $\log V_G$ values on a freshly packed column was measured. The $\log V_G$ values and the coefficients obtained from the regression analysis seem to agree reasonably well, see Table 7.

From the structure of FC-2174, a high percentage of fluorine is present. This is reflected in the negative r-constant (r = -0.275) and by the quite large s-constant (s = 1.828). The small and negative value of r means that the tendency of the phase to interact through n- and π- electrons is almost zero, and the rather high s-constant suggests that the phase is rather dipolar as might be expected of the fluorinated polymer. The ability of the phase to distinguish between homologues in a homologous series is not a dominant factor (l = 0.779), but the hydrogen-bond basicity (a = 2.365) is striking. This a-value is very high for a structure that does not possess any electron donor property. However, 2-3 % of the polymer consists of other compounds that contain phenol and sulfonyl groups, which are very basic. An Infra-Red spectrum obtained by Diffusive Reflectance, see Figure 2, showed that the phase contains OH, with a small broad band at 3600 cm^{-1}, and also has a C=O stretch at 1730 cm^{-1}, a phenolic C-O group at 1300 cm^{-1} and a S=O group identified at 1400 cm^{-1}. This IR result is in accord with the result obtained using the general solvation equation, that hydrogen-bond basicity is present and is due to the groups identified in the IR spectrum. The hydrogen-bond acidity term is not so large, (b = 1.114), and this can be explained as due to the two slight acidic protons in the $-CH_2-CF_2-$ group, and other acidic groups that are present in the polymer.

Once again, the general solvation equation has revealed the presence of active sites in the polymer that are due to rather small quantities of functional groups; in the present case, these functional groups are not included in the notional polymer structure, but arise from other materials in the polymeric solid. And again, results of the general solvation equation have been confirmed by analytical studies on the chemical constitution of the polymer.

Table 7. Fluorel polymers at 298K

Solute	FC-2174 $\log V_G$ 1st	FC-2174 $\log V_G$ 2nd	FLS-2650 $\log V_G$
Heptane	1.478	1.703	1.167
Octane	1.900	2.125	1.568
Nonane	2.296*	2.548	2.051*
Decane	2.708*	2.947	2.444*
Chloroform	2.042	2.267	1.284
1,1,2,2-Tetrachloroethane	3.724	3.949	2.547
1-Chlorobutane	1.913*	2.189	1.560
Trichloroethylene	2.203	2.428	1.754
Tetrachloroethylene	2.522	2.747	2.070
Methylene Iodide	3.413	3.638	2.185
Diethyl ether	1.547	1.772	1.229
Butyl ether	2.785	3.010	2.354
Tetrahydrofurane	2.622*	2.722	2.895*
1,4-dioxane	3.220	3.445	2.562
Butanone	2.640	2.865	3.525
Heptan-2-one	3.800	4.025	3.888
Octan-2-one	4.171	4.396	2.254
Propyl formate	2.463	2.688	3.426*
Pentyl acetate	3.731	3.956	3.292
Butyl propionate	3.629	3.854	2.314
Acetonitrile	2.534	2.759	1.719*
Ethanol	2.428*	2.665	2.771
Propanol	2.812	3.037	3.261
2,2,2-TFE	2.617	2.842	1.534*
1,1,1,3,3,3-HFIP	3.295	3.520	1.594*
2-Methoxyethanol	3.373	3.598	2.863
Toluene	2.655	2.880	2.139
Ethylbenzene	2.966*	3.188	2.407
o-Xylene	3.215	3.440	2.643*
Propylbenzene	3.268*	3.495	2.717*
Butylbenzene	3.635	3.860	3.078
Chlorobenzene	3.011*	3.266	2.456
1,2-Dichlorobenzene	3.802	4.027	3.228*
Iodobenzene	3.780	4.005	2.984
Pyrole	3.619	3.844	2.551

* Standard values.

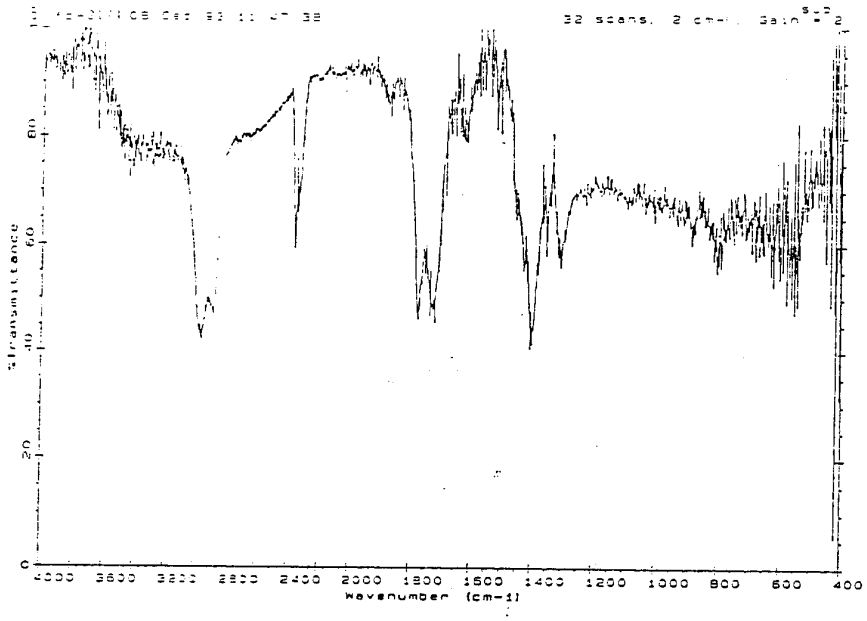

Figure 2 IR spectrum of FC-2174

4.6 Poly(vinylidene fluoride-co-hexafluoropropylene) (Fluorel FLS-2650)

The notional structure of this polymer is the same as FC-2174, FLS-2650 has no other added ingredients, except for tetrafluoroethene (unknown percentage) and the main copolymer; these total 100%. This FLS-2650 polymer was coated onto an inert support of 40-60 mesh at 6.993% loading, and packed into a column of 96cm length, 3.0mm in width, and a packing weight of 4.2646g. Retention volumes for the 34 compounds of the Fluorel FC-2174 set were obtained, Table 7, so that a good comparison could be made. The regressiion equation is,

$$\log V_G = -1.184 - 0.734\ R_2 + 1.186\ \pi^H_2 + 0.626\ \Sigma\alpha^H_2 + 1.335\ \Sigma\beta^H_2 + 0.764\ \log L^{16} \qquad (40)$$

n = 34, r = 0.9889, sd = 0.114, F = 247.1

No bleeding of the column was noticed, but many solute peaks were considerably tailed, especially those for alcohols and bases. A major difference between FLS-2650 and FC-2174 is in the a-constant (0.626 and 2.365 respectively), but we know that the latter large value is due to the presence of other compounds, see above. From the structure of the FLS 2650 polymer, only a weak basicity would be expected, exactly as found.

4.7 Poly(tetrafluoroethylene-co-propylene) (Aflas polymers, 100H, 100S, and 150P)

$$(-CF_2CF_2-)_n(-CH_2-CH[CH_3]-)_m$$

The Aflas polymers, poly(tetrafluoroethylene-co-propylene), 100H, 100S and 150P were iniitially dissolved in THF with the aid of heat by means of refluxing, and then sonicated. The amount that could be coated onto the support was rather low, 3.986%, 5.749% and <4% for 100H, 100S and 150P respectively. The coated Aflas polymer (100H) was packed into a glass column and conditioned at 373K for 24 hours. However, it was found that the Flame Ionisation Detector (FID) was very unstable and showed the behaviour characteristic of a bleeding column; this behaviour continued for a week until it the base line settled down. A set of hydrocarbons was tested, and gave fairly symmetrical peaks, so that a standard could be chosen. With considerable difficulty due to the unstable FID, a few other probes were studied. However, it was noticed that the retention time of the standard greatly decreased during the experimentation. The column was then unpacked, and the weight of the polymer on the packing obtained by ashing. It was found that 40% of the initial weight of the 100H polymer had been lost. Another column of the same material was packed, and exactly the same symtoms were shown. A sample of 100H coated support was thermally analysed, using a Thermal Gravimetric Perkin Elmer apparatus, see Figure 3.

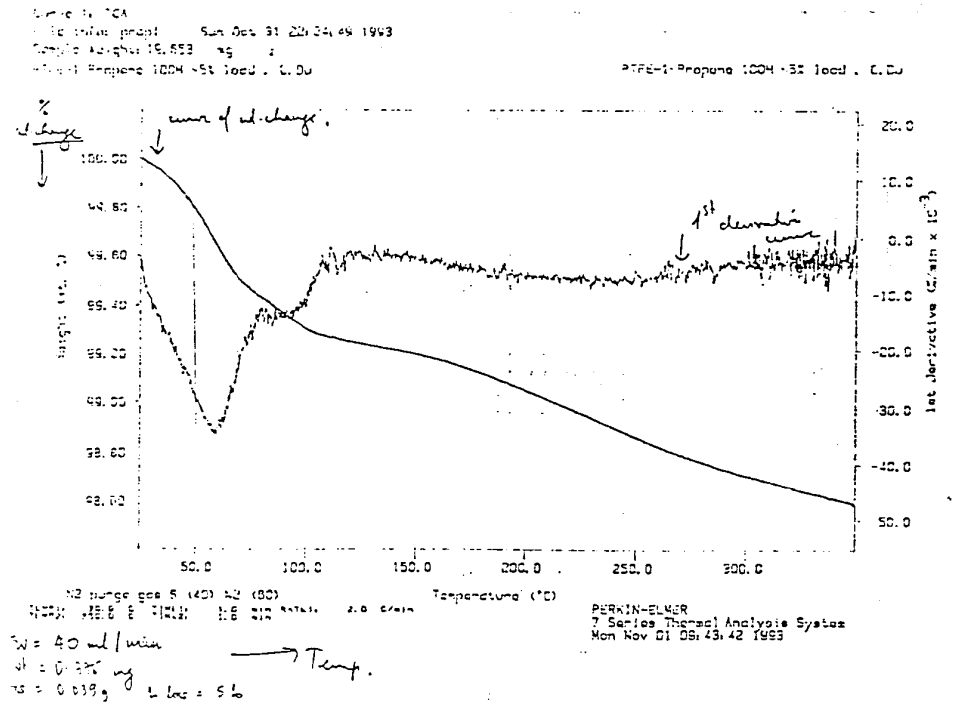

Figure 3 Thermo Gravimetric Plot of Aflas 100H

It is clear that the 100H polymer is thermally unstable when coated onto a support. Possibly, the thermal instability is due to the general procedure of solution (iie. sonication and conditioning (333K). Another Aflas polymer, 150P, also showed column bleeding.

A less vigorous method of dissolving the Aflas polymers was carried out, this time using 1,1,3-trifluorotrichloroethane as a solvent. After leaving the Aflas polymer in the solvent for a very long period of time, the polymer swells. instead of sonicating to dissolve the polymer, this time the mixture of polymer and solvent was gently stirred using a glass rod. This process takes longer in time, but it is believed that the sonication used before broke up polymer. In addition, the high temperature used in conditioning may also have contributed to break up of the polymer.

The 100H polymer, as a solution in the 1,1,3-trifluorotrichloroethane, was coated onto chromosorb of 60/80 mesh size with a percentage loading of 3.421%, and the solvent was taken off in a vacumn dessicator. The coated support was packed into a column of 95cm length and a width of 2.0mm; the packing weighed 3.4903g. The packed column was conditioned at a much lower temperature than previously, ~303K.

After the new method of preparing the stationary phase, we were able to examine 41 solutes on 100H and 100S, see Table 8; most of the solutes gave rise to sharp peaks with little tailing. The regression equation for 100H is,

$$\log V_G = -0.101 + 0.273\ R_2 + 1.477\ \Sigma\alpha^H_2 + 0.895\ \Sigma\beta^H_2 + 0.874\ \log L^{16} \quad (41)$$

n = 41, r = 0.9912, sd = 0.111, F = 504.2

The 100H polymer has no dipolarity/polarizability, and is a moderate hydrogen-bond acid (b = 0.895) as expected from the structure. What is unexpected is the large basicity (a = 1.477). Examination of the solid by diffuse reflectance FTIR showed the presence of a small amount of OH but this is hardly enough to explain the large a-constant.

Aflas polymer 100S was coated in the same way as the 100H polymer. 100S with a percentage loading of 3.8214% was packed into a column of length 96.5cm and width 2.0mm; the packing weighed 3.6529g. The results in Table 7 for polymer 100S were treated as usual to yield,

$$\log V_G = -0.270 + 0.504\ \pi^H_2 + 1.460\ \Sigma\alpha^H_2 + 0.653\ \Sigma\beta^H_2 + 0.912\ \log L^{16} \quad (42)$$

n = 41, r = 0.9941, sd = 0.098, F = 750.4

Again, the polymer exhibits a considerable degree of hydrogen-bond basicity (a = 1.460) which we feel must be due to elements such as oxygen in the polymer.

Table 8. Poly(tetrafluoroethylene-co-propylene) polymers at 298K

Solute	100H $logV_G$	100S $logV_G$
Heptane	2.551	2.627
Octane	3.052*	3.098*
Nonane	3.544*	3.574*
Decane	4.017	4.050*
Chloroform	2.307	2.402
1,1,2,2-Tetrachloroethane	3.858	3.930
Trichloroethylene	2.691	2.758
Diiodomethane	3.870*	3.938
Diethylether	2.180	2.063
Isobutylether	3.093	3.093
Tetrahydrofuran	2.833	2.758
1,4-Dioxane	3.208*	3.111
Butanone	2.700	2.437
Pentan-3-one	2.907*	2.958*
Heptan-2-one	3.807	3.837
Octan-2-one	4.257	4.256
sec-Butyl acetate	3.051*	3.074
n-Pentyl acetate	3.851	3.817*
n-Butyl propanoate	3.747	3.720
Acetonitrile	1.953	1.957
Methylamine	2.044	2.029
N,N-dimethylformamide	3.739	3.712
Methanol	1.953	1.613
2-Methylpropan-2-ol	2.911	2.495*
Pentanol	3.659	3.513
Hexanol	4.016	4.066
2,2,2-Trifluoroethanol	2.077	1.969
1,1,1,3,3,3-Hexafluoropropan-2-ol	2.500	2.689
2-Methoxyethanol	3.176	3.263
Ethane-1,2-diols	4.182	3.991
Dimethylsulfoxide	3.959	4.433
Toluene	2.996	3.071*
o-Xylene	3.612*	3.656
Propylbenzene	3.847	3.875*
Chlorobenzene	3.395*	3.457*
1,2-Dichlorobenzene	4.187	4.346
Iodobenzene	4.330	4.378
Anisole	3.769	3.816*
Phenol	4.626	4.626
m-Cresol	5.022	5.125
4-Fluorophenol	4.674	4.880
Pyridine	3.405	3.368

* Standard values

4.8 Conclusions on the IGC of polymers by GLC

As found in the adsorption work, the solvation equation indicated that the various polymers studied all had more acidic or basic properties than expected from their structure. In part this might be due to adsorption on the support when using stationary phases with only small % loadings. However, in the case of FC-2174, with a 12% loading, this is less likely to occur, and the large basicity of the polymer must be due to other compounds present (2-3%). The diffuse reflectance IR seems to confirm this. Again, we suggest that examination of the polymers by IR and other techniques is advisable, in order to detect other additives or impurities that might affect the solubility properties of the polymers. A summary of the characteristic for polymers by GLC is in Table 9.

Table 9. Inverse Gas-chromatography of Liquid Phases at 298K

Phases	c	r	s	a	b	l	n	R	sd	F
Chromosorb GAW-DMCS(40-60)	-2.430	-0.297	0.351	2.131	2.048	0.695	22	0.9650	0.144	43.3
rubber (388P)	-0.932	0.226	-	0.261	0.349	1.119	42	0.9961	0.068	1187.0
rubber (B178)	-1.276	0.260	-	0.326	0.415	1.146	42	0.9956	0.074	1050.7
rubber (B174)	-0.975	0.283	-	0.333	0.557	1.076	42	0.9917	0.098	548.7
Epom 'Nordel' rubber	-0.154	0.204	-	0.389	0.206	0.943	42	0.9950	0.063	931.1
FC-2174	-0.937	-0.275	1.828	2.365	1.114	0.779	34	0.9948	0.078	536.5
FLS-2650	-0.184	-0.734	1.886	0.626	1.335	0.764	34	0.9889	0.114	247.1
Aflas(100H)	-0.101	-	0.273	1.477	0.895	0.874	41	0.9912	0.111	504.2
Aflas (100S)	-0.270	-	0.504	1.460	0.653	0.912	41	0.9941	0.098	750.4
Aflas 150P	Not measurable due to column bleeding									

5. Vapor Pressure Estimation

5.1 Introduction

The use of gas-liquid chromatography, GLC, in the estimation of vapor pressures has been practiced for some time, eg [14,15] The general method is to obtain GLC retention data for a series of compounds of known vapor pressure on a given stationary phase, and then hope to correlate the retention data and vapor pressure through an equation of the form:

$$\log t,T2 = c - \log P^{o},T1 \qquad (43)$$

In eq(43), t can be just the retention time of a compound, relative to a particular standard, on a given stationary phase at a temperature T2, and P^{o} is the corresponding vapor pressure at a temperature T1. It is not necessary for T2 to equal T1, and, indeed, usually T2 will be an elevated temperature, whereas T1 will be some ambient temperature.

There are a number of advantages in being able to estimate vapor pressures via eq(43). The method is quick and convenient, does not require the compound to be pure, and uses only very small quantities. On the other hand, there is a considerable practical difficulty in that a knowledge of reliable vapor pressures is needed in order to be able to set up the equation. In addition, the GLC stationary phase has to be chosen with some care. Usually a non-polar phase, or a phase of limited polarity, will work best for compounds that are themselves not too polar. In the present work, we started with an Apiezon coated capillary column, as an example of a phase that is rather, but not entirely, non-polar. In addition, we have also used a conventional packed Apiezon column in order to compare results.

5.2 Experimental discussion on capillary GLC

The Gas Chromatograph used with the capillary columns was a Carlo Erba 'Fractovap Linea 2150', equiped with a split device. In this system, the solute is injected into the carrier gas stream as usual, but the carrier gas is then split at a T-junction so that only a small proportion of the gas mixture (solute plus carrier gas) is allowed to enter the column, the rest being vented out of the system. The split ratio can be set as required, through an adjustment valve in the split device. However, the split ratio has to be determined by measurement of the flow rate through the column, and the flow rate of the vented gas stream.

5.2.1 Measurement of flow rates

Since the Carlo Erba chromatograph, as is general in capillary work, is fitted with a flame ionisation detector, the flow rate through the column has to be obtained as the outlet flow rate, when the flame is extinguished. The hydrogen flow is turned off, and a flexible tube is attached to the end of the detector, which in turn is close-fitted to the outlet end of the capillary column. Since the capillary flow rates are very small, ordinary flow meters cannot be used, and it was necessary to construct a

small-sized soap bubble flow meter of 3 mm id, and of 1 ml total volume. We shall refer to this as the capillary flow meter.

After optimal conditions had been worked out, especially the nitrogen flow rate and the relative split ratio using the split ratio adjustment valve, the absolute split ratio was determined as follows. The hydrogen flow was turned off, and the column outlet flow obtained using the capillary bubble meter. At the same time, the flow rate of the vented gas stream out of the split device was obtained using an ordinary 10 ml soap bubble meter. With both bubble meters, flow rates were determined using a stop watch, and several measurements were made on each occasion.

5.2.2 Experimental conditions with the Apiezon column

The capillary column used was a fused silica Supelco Apiezon L column, of 0.53 mm id, and of 15 m length. It was purged with pure nitrogen for one hour at room temperature, and then conditioned at 470K for two hours prior to use at 423 or 353K. Results refer to the following experimental conditions. Those for determinations at 353K are the same as those at 423K, except where shown.

Supelco column number	936401F	
Phase	Apiezon L	
Film thickness	0.50 microns	
Column diameter	0.53 mm id	
Column length	15 m	
Column temperature	423K	353K
Injecter temperature	493K	
Detector temperature	493K	
Carrier gas	Nitrogen	
Nitrogen pressure	0.5 Kg/cm^2	
Hydrogen pressure	0.5 Kg/cm^2	
Air pressure	1.6 Kg/cm^2	
Range	10	
Attenuation	1.0	
Chart speed	10 mm/min	
Split ratio	160:1	100:2
Flow rate	0.027 ml/s	0.091 ml/s
Inlet pressure	796 mmHg	837 mmHg
Outlet pressure	761 mmHg	765 mmHg
Phase density	0.810 g/ml	0.838 g/ml
Phase volume	0.013 ml	0.012 ml

5.3 Results with Apiezon columns

Absolute retention data, as logL values were determined on the Apiezon coated capillary column at 423K and at 353K, and on a conventional packed column at 353K, with a 15.5% loading of Apiezon. Results are in Table 10, where we can compare the two sets of data at 423K. By inspection, the values on the packed column and capillary column are very close.

Table 10. Comparison of absolute logL values on Apiezon at 423K and at 353K with values of -logP/atm at 298K

Solute	Packed 423K	Capillary 423K	Capillary 353K	-logP 298K
Octane	1.555	1.547	2.241	1.733
Nonane	1.809	1.769	2.593	2.239
Decane	2.050	2.009	2.935	2.742
Undecane	2.305	2.279	3.303	3.242
Dodecane	2.568	2.517	3.648	3.737
Tetradecane	3.078	3.009	4.343	4.901
Heptan-2-one	1.719	1.713	2.417	2.295
Nonane-2-one	2.249	2.190	3.009	3.182
Decane-2-one	2.503	2.399	3.451	3.636
Cyclopentanone	1.533	1.301	2.116	1.833
Cyclohexanone	1.834	1.699	2.447	2.272
Pentyl acetate	1.637	1.636	2.420	2.274
Dimethyl malonate	1.668	1.491	2.292	2.987
Diethyl malonate	1.992	1.859	2.764	3.559
Benzene	1.254	1.477	1.639	0.902
Toluene	1.573	1.636	2.130	1.426
Ethylbenzene	1.808	1.845	2.468	1.901
Propylbenzene	2.026	2.016	2.785	2.351
Butylbenzene	2.284	2.028	3.149	2.868
Benzyl alcohol	2.277	2.083	2.935	3.919
Pyridine		1.757	1.929	1.567
2-Chloroethyl-isoamylsulfide		2.462	3.501	3.801

An exact comparison between the two data sets is given by eq(44),

$$\log L(\text{cap},423) = 0.115 + 0.912\ \log L(\text{pack},423) \qquad (44)$$

$n = 20, \quad r = 0.9680, \quad sd = 0.11, \quad F = 267.9$

As can be seen from Figure 4, benzene (B) is outlier, probably because of its very short retention times at 423K. If benzene is left out, the correspondence is improved,

$$\log L(\text{cap},423) = -0.009 + 0.967\ \log L(\text{pack},423) \qquad (45)$$

$n = 19, \quad r = 0.9760, \quad sd = 0.09, \quad F = 341.3$

It seems from eq(44) and (45) that there is no particular advantage to be gained by the use of capillary over packed columns at elevated temperature. Indeed, if absolute retention data are needed, then packed columns are to be preferred, because of the difficulty in obtaining absolute data on capillary columns.

We can now compare the obtained logL values on the two columns with the set of standard vapor pressures listed in Table 10. These have been taken from authoritative sources [16-23], and refer to vapor pressures in atmospheres at 298K. Note that the

vapor pressures are all given as -logP/atm. A plot of -logP at 298K against logL(pack) at 423K is shown in Figure 5. The corresponding regression equation is,

$$-\log P = -1.296 + 2.012 \log L(\text{pack},423) \qquad (46)$$

n = 20, r = 0.9106, sd = 0.41, F = 87.3

Both Figure 5 and eq(46) show that a general equation cannot yield estimated logP values to better than 0.4 log units. However, it is clear from Figure 5, and from Figures 6-8, that the three solutes benzyl alcohol (A), dimethylmalonate (M) and diethyl malonate (E) fall off the normal line. If these three solutes are removed we find,

$$-\log P = -1.500 + 2.043 \log L(\text{pack},423) \qquad (47)$$

n = 17, r = 0.9764, sd = 0.22, F = 307.1

Eq(47) could be used to obtain logP values in general for compounds, providing that alcohols and malonates are excluded. A quite similar result is obtained with the capillary column at 423K, as shown by Figure 6. The corresponding equation is,

$$-\log P = -1.194 + 2.004 \log L(\text{cap},423) \qquad (48)$$

n = 22, r = 0.8374, sd = 0.55, F = 47.0

which is even worse than eq(46). If the same three points are removed, then,

$$-\log P = -1.691 + 2.173 \log L(\text{cap},423) \qquad (49)$$

n = 19, r = 0.9396, sd = 0.35, F = 128.1

The equations using the capillary column are not as good as those with the packed column, so that again there seems to be no real advantage in using capillary columns.

One of the reasons for the rather poor correlations, above, might be the differential heat of solution of solutes in Apiezon, as between 298 and 423K. We therefore studied the capillary column at 353K, about as low a temperature as it is possible to go, and still deal with the less volatile compounds. The absolute values of the retention data are in Table 10. A plot of -logP vs logL is in Figure 7, and the corresponding equation is,

$$-\log P = -1.141 + 1.396 \log L(\text{cap},353) \qquad (50)$$

n = 22, r = 0.9097, sd = 0.42, F = 95.7

Once again, if the three above points are removed, the correlation improves to,

$$-\log P = -1.376 + 1.429 \log L(\text{cap},353) \qquad (51)$$

n = 19, r = 0.9833, sd = 0.18, F = 497.0

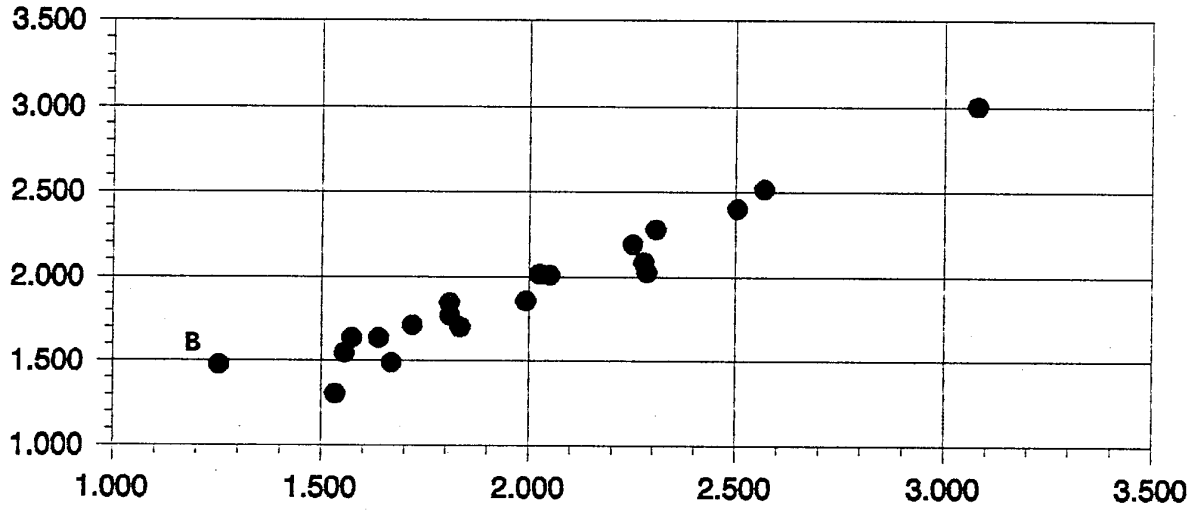
Plot of logL on Apiezon at 423K
Capillary vs Packed Column
3.500
3.000
2.500
2.000
1.500
1.000
B
1.000
1.500
2.000
2.500
3.000
3.500

Figure 4.

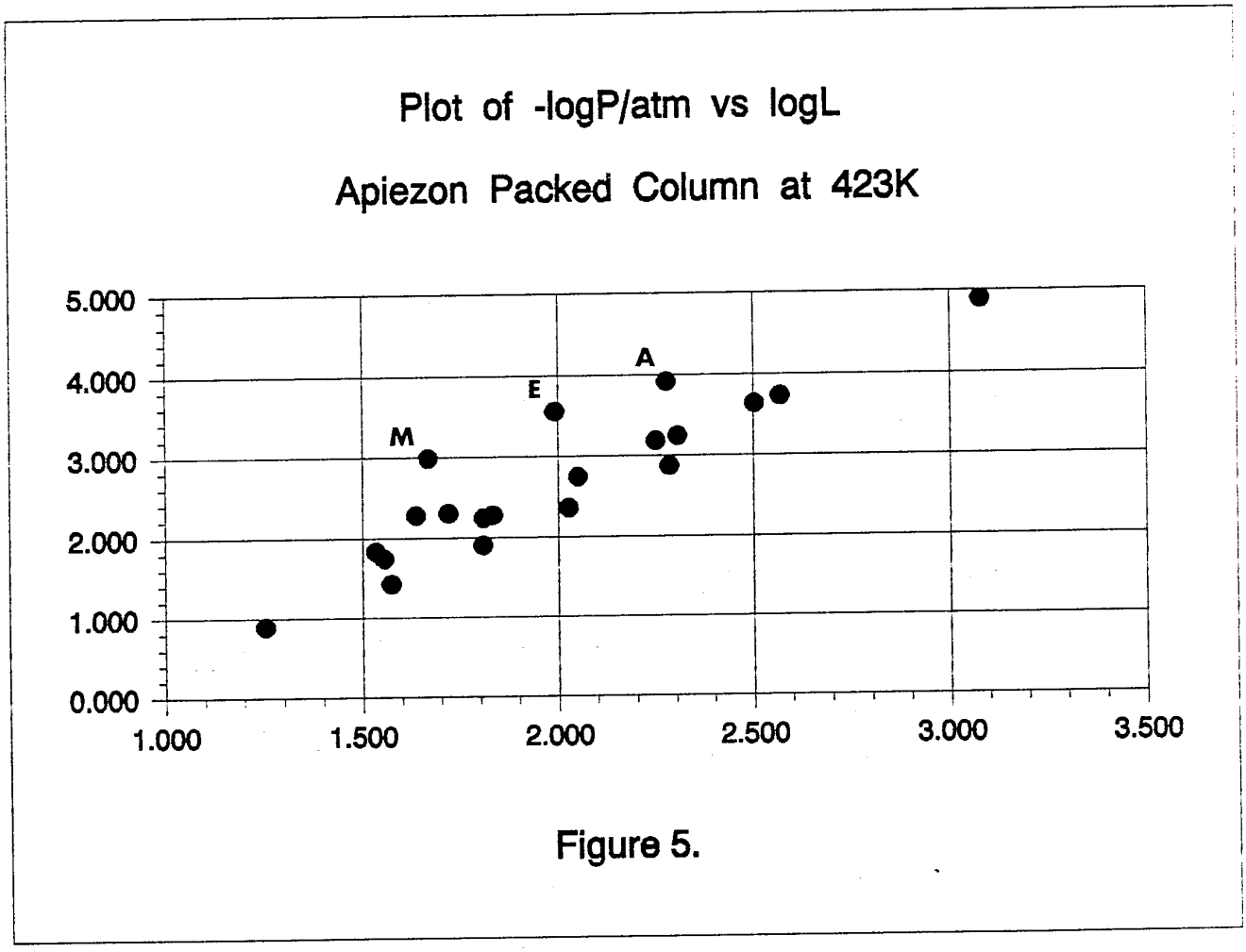
Plot of -logP/atm vs logL
Apiezon Packed Column at 423K
5.000
4.000
3.000
2.000
1.000
0.000
1.000
1.500
2.000
2.500
3.000
3.500
A
E
M

Figure 5.

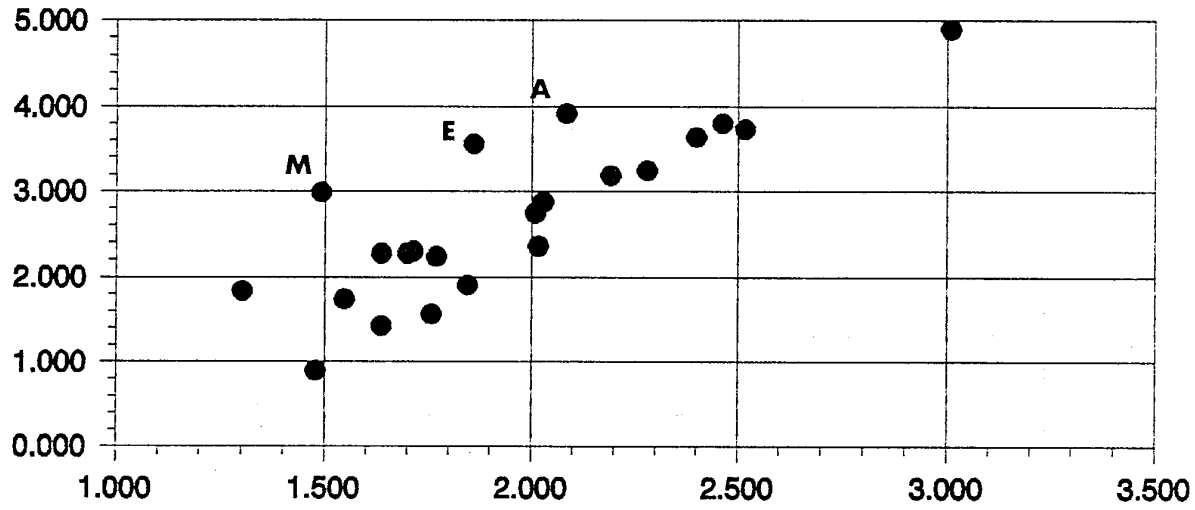
Plot of -logP/atm vs logL
Apiezon Capillary Column at 423K
5.000
4.000
3.000
2.000
1.000
0.000
1.000
1.500
2.000
2.500
3.000
3.500
A
E
M

Figure 6.

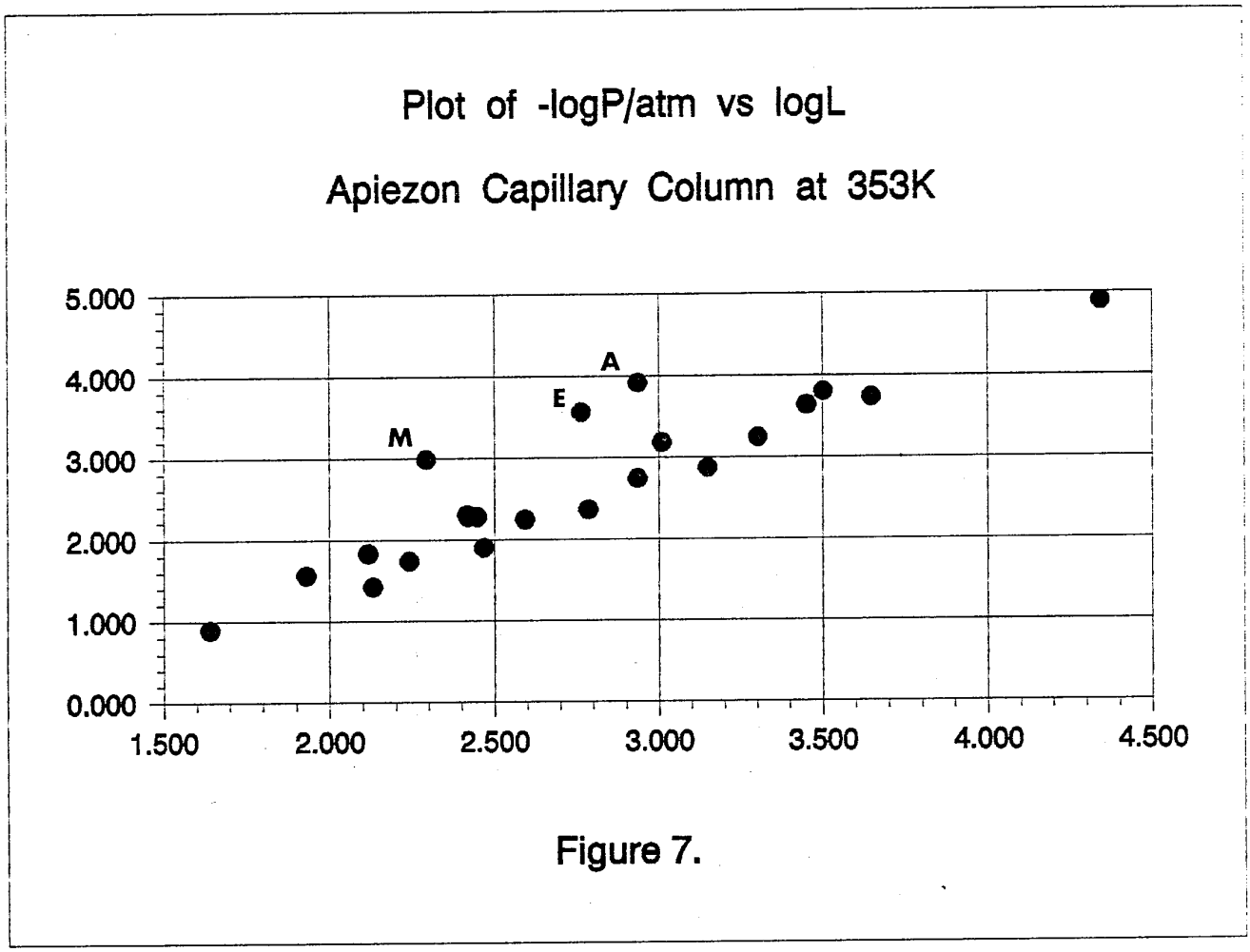
Plot of -logP/atm vs logL
Apiezon Capillary Column at 353K
5.000
4.000
3.000
2.000
1.000
0.000
1.500
2.000
2.500
3.000
3.500
4.000
4.500
A
E
M

Figure 7.

Our conclusion is that logP values at 298K might be estimated to around 0.2 log unit, using a packed Apiezon column at 423K or a capillary Apiezon column at 353K. Possibly, a packed Apiezon column at 353K might perform slightly better. In any case, no general correlation equation can be formulated, since different types of solute seem to lie on different lines. The above equations are definately unsuitable for the estimation of logP values for malonates. At the moment, the best that can be done is to use the two points for dimethylmalonate and diethylmalonate. The single sulfide for which we have reliable logP data [22] is no better correlated with the 423 results than with the 353K results. An estimated logP/atm value from eq(49) is -3.66, and from eq(51) is 3.63, as compared to the measured value of -3.80 units. Were a few more logP values available for sulfides and malonates, it would be possible to construct separate equations for these series, and to estimate logP more accurately.

5.4 Results with a poly(dimethylsiloxane) column

Since the correlations between vapor pressure and retention data were not very good with the Apiezon columns, we studied another nonpolar column, poly(dimethylsiloxane), that we refer to as PDMS, but trade names are SE30 and OV1. A capillary column was used at 353K in preference to a higher temperature, following on from the Apiezon results at 353 and 423K. Details of the experimental conditions are below,

Supelco column number	935110
Phase	PDMS
Film thickness	1.20 microns
Column diameter	0.53 mm id
Column length	10 m
Column temperature	353K
Injecter temperature	493K
Detector temperature	493K
Carrier gas	Nitrogen
Nitrogen pressure	0.5 Kg/cm^2
Hydrogen pressure	0.5 Kg/cm^2
Air pressure	1.6 Kg/cm^2
Range	10
Attenuation	1.0
Chart speed	10 mm/min
Split ratio	200:1
Flow rate	0.044 ml/s
Inlet pressure	798 mmHg
Outlet pressure	765 mmHg
Phase density	1.000 g/ml
Phase volume	0.020 ml

Absolute logL values were obtained in the same way for the 22 solute set, and are given in Table 11.

Table 11. Comparison of absolute logL values on poly(dimethylsiloxane) at 353K with values of -logP/atm at 298K

Solute	logL	-logP
Octane	1.858	1.733
Nonane	2.172	2.239
Decane	2.491	2.742
Undecane	2.803	3.242
Dodecane	3.116	3.737
Tetradecane	3.723	4.901
Heptan-2-one	2.088	2.295
Nonane-2-one	2.713	3.182
Decane-2-one	3.009	3.636
Cyclopentanone	1.733	1.833
Cyclohexanone	2.108	2.272
Pentyl acetate	2.169	2.274
Dimethyl malonate	2.147	2.987
Diethyl malonate	2.604	3.559
Benzene	1.467	0.902
Toluene	1.768	1.426
Ethyl benzene	2.044	1.901
Propyl benzene	2.318	2.351
Butyl benzene	2.624	2.868
Benzyl alcohol	2.512	3.919
Pyridine	1.646	1.567
2-Chloroethyl-isoamylsulfide	2.974	3.801

If data for all the 22 solutes are used, the following regression equation is found, see also Figure 8,

$$-\log P = -1.280 + 1.680\ \log L(PDMS,353) \qquad (52)$$

$n = 22,\quad r = 0.9440,\quad sd = 0.33,\quad F = 163.7$

This is appreciably better than the Apiezon equations for the full data set, and if the three compounds as above are left out (the two malonates and benzyl alcohol), we find,

$$-\log P = -1.344 + 1.661\ \log L(PDMS,353) \qquad (53)$$

$n = 19,\quad r = 0.9897,\quad sd = 0.15,\quad F = 816.2$

Again, this is better than the corresponding equations with the Apiezon columns, eq(47, 49, and 51), with a lower standard deviation in -logP of 0.15 units. This suggests that in general the PDMS capillary column at 353K might be useful in the estimation of logP values at 298K. However, as before, the two malonates are excluded, and a separate equation would have to be set up. In addition, the predicted -logP value for the only sulfide in the data set, 2-chloroethyl-isoamylsulfide, is 3.60 on eq(53), and 3.63 or 3.66 from the Apiezon capillary column, so that the PDMS column is no better in this respect.

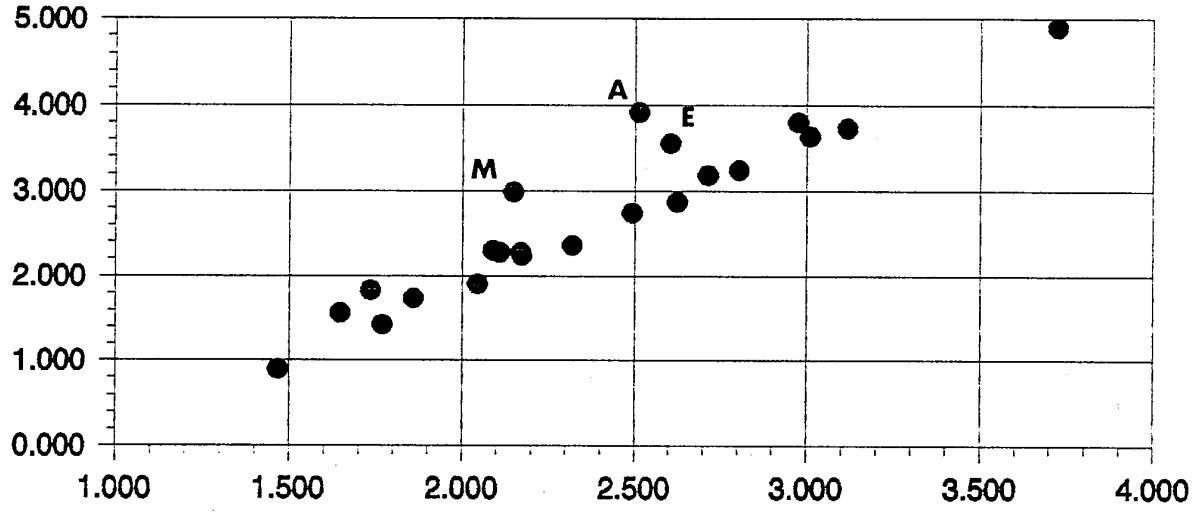
Plot of -logP/atm vs logL
PDMS Capillary Column at 353K
5.000
4.000
3.000
2.000
1.000
0.000
1.000
1.500
2.000
2.500
3.000
3.500
4.000
A
E
M

Figure 8.

5.5 Conclusions on the vapor pressure estimations

From the results we have on the Apiezon and PDMS columns, it is quite clear that no logP vs logL equation can be constructed that covers a range of classes of compound. In more general terms, no one equation can be set up between GLC retention data and vapor pressure. The best that can be done is to construct equations for selected classes of compound, but this requires a knowledge of vapor pressure for standard compounds. As regards the malonates, we have obtained -logP for diethylmalonate from vapor pressure data supplied by Shuely [22], and find that -logP/atm = 3.56 at 298K. Existing vapor pressure /temperature equations listed by Stephenson and Malanowski [24] yield values of 3.32 and 3.90 for -logP, on extrapolation from higher temperature. Although these span the preferred value of Shuely, the difference between the two values, 0.58 log units, illustrates the difficulty in getting reliable values. The value we quote for dimethylmalonate, -logP/atm = 2.99 at 298K, is derived by extrapolation from the vapor pressure - temperature equation of Askonas and Daubert [21], and cannot really be used as a standard. Thus in order to make any headway in estimation of vapor pressures for malonates, it will be essential to have a good value for dimethylmalonate at 298K, that can be used as a standard.

The position with the chlorosulfides is not so bad, because the one compound we have been able to look at, 2-chloroethyl-isoamylsulfide, fits our equations much better than do the malonates. Thus, our calculated -logP/atm values are 3.66 from eq(49), 3.63 from eq(51), and 3.60 from eq(53), as compared to the determined value of 3.80 [22]. But note that the latter value is actually an extrapolated one, see Table 12 below. It would certainly be possible to set up an Apiezon column, either a packed column or a capillary column, that could be used to estimate vapor pressures of sulfides, especially if one or two other sulfides were available as check compounds.

5.6 Vapor pressure of 2-chloroethyl-isoamylsulfide and diethylmalonate

From vapor pressure determinations at various temperatures, supplied by Dr Shuely, we constructed equations of the Antoine type, where P is in mmHg and T is the absolute temperature. Note the use of natural logs in eq(54).

$$\ln[P_{mmHg}] = A - B/T \qquad (54)$$

In the case of 2-chloroethyl-isoamylsulfide, there were available [22] nine pairs of vapor pressure/temperature values, see Table 12, that we fitted to the equation,

$$\ln[P_{mmHg\ for\ chloroethylsulfide}] = 23.4633 - 7628.826/T \qquad (55)$$

$n = 9, \quad r = 0.99922$

The calculated values on eq(55) are in Table 12, at various temperatures, including some for which Shuely [22] had calculated values. Eq(55) reproduces the nine observed values very well.

Table 12. Vapor pressure of 2-chloroethyl-isoamylsulfide

t°C	T/K	Pmm (obs)	Pmm (calc, eq 55)	Pmm (calc, ref 22)
20.0	293.2		0.0776	
25.0	298.2		0.1201	
30.0	303.2		0.183	0.173
35.0	308.2		0.275	0.271
55.0	328.2		1.245	1.305
55.9	329.1	1.3	1.326	
58.9	332.1	1.7	1.635	
60.0	333.2		1.764	1.845
68.2	341.4	3.0	3.058	
70.0	343.2		3.438	3.523
72.0	345.2	4.0	3.910	
76.6	349.8	5.0	5.229	
78.9	352.1	6.0	6.030	
81.8	355.0	7.1	7.197	
83.2	356.4	8.0	7.831	
85.2	358.4	9.0	8.825	
90.0	363.2		11.69	10.93
100	373.2		20.52	18.01

For diethylmalonate, we did not use all the data supplied, but restricted our analysis to temperatures near ambient, in order to interpolate lnP at or near to 298K. The data we used for diethylmalonate is in Table 13, together with the calculated values from the fitting equation,

$$\ln[P/\text{mmHg for diethylmalonate}] = 21.6667 - 6926.592/T \qquad (56)$$

$n = 6, \quad r = 0.999998$

Since the observed [22] values span ambient temperature, the 298K value we have used is obtained by interpolation, rather than by extrapolation from higher temperature.

Table 13. Vapor pressure of diethylmalonate

t°C	T/K	Pmm (obs)	Pmm (calc, eq 56)
9.7	282.9	0.060	0.060
11.4	284.6	0.069	0.069
14.8	288.0	0.092	0.092
20.0	293.2		0.141
25.0	298.2		0.210
64.2	337.4	3.1	3.12
64.6	337.8	3.2	3.20
66.5	339.7	3.6	3.58

6. Determination of Descriptors

We have taken the opportunity of the availability of the capillary and the packed Apiezon columns, and the capillary PDMS column to determine logL values for a wide variety of solutes. Although the additional solutes to those in Tables 10 and 11 are not suitable for use in logP/logL correlations, they are valuable in constructing regression equations between $logL^{16}$ and logL. Once these have been set out, it then becomes possible to back-calculate a large number of hitherto unknown $logL^{16}$ values for important compounds such as the chloroalkylsulfides and the malonates. A large set of solutes, see Table 14, was examined on the Apiezon capillary column at 423K, leading to the regression equation,

$$logL(cap\ AP,\ 423) = -\ 0.079 + 0.294\ R_2 + 0.457\ logL^{16} \qquad (57)$$

$$n = 85,\quad r = 0.9916,\quad sd = 0.072,\quad F = 2407$$

Because the equation contains only terms in R_2 and $logL^{16}$, the latter can be back-calculated for any solute examined. A similar study was carried out using the packed Apiezon column at 423K; the retention data are in Table 15, and lead to the equation,

$$logL(pack\ AP,\ 423) = -\ 0.442 + 0.256\ R_2 + 0.164\ \pi_2^H + 0.307\ \Sigma\alpha_2^H + 0.531\ logL^{16} \qquad (58)$$

$$n = 59,\quad r = 0.9975,\quad sd = 0.037,\quad F = 2341$$

Eq(58) is quite a bit better than eq(57), but because of the additional terms in π_2^H and $\Sigma\alpha_2^H$ that occur in equation (58), it is necessary to determine these parameters before back calculation of $logL^{16}$ can be carried out (except for a few compounds). In order to obtain more accurate data on small compounds, we also studied a range of compounds on the capillary Apiezon column and the capillary PDMS column at 353K; results are in Table 16 and lead to the regression equations,

$$logL(cap\ AP,\ 353) = -\ 0.436 + 0.165\ \pi_2^H + 0.419\ \Sigma\alpha_2^H + 0.710\ logL^{16} \qquad (59)$$

$$n = 66,\quad r = 0.9953,\quad sd = 0.062,\quad F = 1604$$

This equation is comparable to equation (57) as regards goodness-of-fit, but does need a knowledge of the π_2^H and the $\Sigma\alpha_2^H$ descriptors before $logL^{16}$ can be calculated.

$$logL(cap\ PDMS,\ 353) = -\ 0.301 + 0.143\ \pi_2^H + 0.434\ \Sigma\alpha_2^H + 0.600\ logL^{16} \qquad (60)$$

$$n = 69,\quad r = 0.9957,\quad sd = 0.052,\quad F = 2490$$

The equations at 353K, eq(59) and eq(60) are of about the same quality as those at 423K, but again need a knowledge of π_2^H and $\Sigma\alpha_2^H$ before $logL^{16}$ can be calculated.

Table 14. Values of logL on the Apiezon capillary column at 423K

Compound	LogL
n-Pentane	0.945
n-Hexane	1.070
n-Octane	1.547
n-Nonane	1.769
n-Decane	2.009
n-Undecane	2.279
n-Dodecane	2.517
n-Tridecane	2.748
n-Tetradecane	3.009
n-Pentadecane	3.245
n-Hexadecane	3.489
n-Heptadecane	3.716
n-Octadecane	3.957
Cyclohexane	1.287
Oct-2-ene	1.742
Dodec-1-ene	2.490
Cyclooctene	1.997
Tetrachloromethane	1.193
1,1,2,2-Tetrachloroethane	1.819
1-Chlorobutane	1.163
1-Chloropentane	1.405
1-Bromobutane	1.560
Dibutylether	1.888
1,4-Dioxan	1.520
Butanone	1.000
4-Methylpentan-2-one	1.477
Heptan-2-one	1.713
Heptan-3-one	1.713
2,4-Dimethylpentan-3-one	1.414
Octan-2-one	1.968
Nonan-2-one	2.190
Nonan-5-one	2.083
Decan-2-one	2.399
Cyclohexanone	1.699
Propyl formate	1.262
Pentyl acetate	1.636
n-Butyl propanoate	1.721
Ethyl acetoacetate	1.616
Diethyl malonate	1.859
Dimethylformamide	1.576
Dimethylacetamide	1.672
Heptan-1-ol	1.858
Octan-1-ol	2.083
Octan-2-ol	1.951
Decan-1-ol	2.420
Cyclohexanol	1.672
Cyclooctanol	2.421
2-Chloroethylethylsulfide	1.859
2-Chloroethyl-n-propylsulfide	2.093
2-Chloroetyl-n-butylsulfide	2.227
Dimethylsulfoxide	1.576
Triethylphosphate	2.002

Benzene	1.477
Toluene	1.636
Ethylbenzene	1.845
n-Propylbenzene	2.016
1,2,3,-Trimethylbenzene	2.216
1,3,5-Trimethylbenzene	2.066
3-Ethyltoluene	2.028
tert-Butylbenzene	2.041
1,2,3,4-Tetramethylbenzene	2.528
1-Phenylhexane	2.686
1,3-Dichlorobenzene	2.223
3-Chlorotoluene	2.022
4-Chlorotoluene	2.051
4-Bromotoluene	2.251
Iodobenzene	2.317
1,3-Dimethoxybenzene	2.426
Methylphenylketone	2.192
Propiophenone	2.461
Benzylmethylketone	2.292
Methyl benzoate	2.221
Phenol	1.903
m-Cresol	2.167
2,4,6-Trimethylphenol	2.550
3-Ethylphenol	2.276
2-Isopropylphenol	2.441
3-Isopropylphenol	2.505
4-Fluorophenol	1.958
2-Chlorophenol	2.092
2,6-Dichlorophenol	2.586
4-Chloro-3-methylphenol	2.731
Benzyl alcohol	2.083
3-Ethylpyridine	2.099
2-N,N-Dimethylaminopyridine	2.329

Table 15. Values of logL on the Apiezon packed column at 423K

Compound	LogL
n-Octane	1.555
n-Nonane	1.809
n-Decane	2.050
n-Undecane	2.305
n-Dodecane	2.568
n-Tetradecane	3.078
Oct-1-ene	1.512
Oct-2-ene	1.603
Tetrachloromethane	1.254
1-Chlorobutane	1.061
1-Chloropentane	1.476
1-Bromopentane	1.687
1,2-Dimethoxyethane	1.020
Heptan-2-one	1.719
Heptan-3-one	1.728
Heptan-4-one	1.680
Nonan-2-one	2.249
Nonan-3-one	2.242
2,6-Dimethylheptan-4-one	1.939
Decan-2-one	2.503
Cyclopentanone	1.533
Cyclohexanone	1.834
sec-Butyl acetate	1.259
tert-Butyl acetate	1.061
Pentyl acetate	1.637
Methyl trimethylacetate	1.207
Dimethylformamide	1.516
Dimethylacetamide	1.777
Heptan-1-ol	1.976
Decan-1-ol	2.773
Cyclohexanol	1.883
Cyclooctanol	2.575
Dimethylsulfoxide	1.889
Benzene	1.254
Toluene	1.573
Ethylbenzene	1.808
n-Propylbenzene	2.026
1,2,3-Trimethylbenzene	2.251
1,3,5-Trimethylbenzene	2.118
3-Ethyltoluene	2.073
n-Butylbenzene	2.284
tert-Butylbenzene	2.125
1,2,3,4-Tetramethylbenzene	2.583
1-Phenylhexane	2.778
1,3-Dichlorobenzene	2.263
3-Chlorotoluene	2.084
4-Chlorotoluene	2.099
2-Bromotoluene	2.345
Iodobenzene	2.385
Methylphenylether	1.950
Methylphenylketone	2.311
Propiophenone	2.556
Phenol	2.110

m-Cresol	2.408
3-Ethylphenol	2.618
2-Chlorophenol	2.205
Benzyl alcohol	2.277
2-Methoxypyridine	1.794
Pyrrole	1.392

Table 16. Values of logL on the Apiezon and PDMS capillary columns at 353K

Compound	LogL Apiezon	LogL PDMS
n-Octane	2.241	1.858
n-Nonane	2.593	2.172
n-Decane	2.935	2.491
n-Undecane	3.303	2.803
n-Dodecane	3.648	3.116
n-Tridecane	4.014	3.421
n-Tetradecane	4.343	3.723
Camphene		2.320
Norbornane		1.703
Norbornylene		1.636
a-Pinene		2.305
Tetrachloromethane	1.788	
trans-Decalin		2.640
cis-Decalin		2.765
Ethyl fluoroacetate		1.471
3-Chloropropyl thioacetate		2.717
Bis(2-chloroethyl)disulfide		3.471
Dibutyl chloromethylphosphonate		4.058
2-Chloroethylmethylsulfide		1.956
2-Chloroethylethylsulfide		2.171
2-Chloroethyl-n-propylsulfide		2.472
2-Chloroethyl-n-butylsulfide		2.642
2-Chloroethyl-isoamylsulfide		2.974
Di-tert-butyldisulfide		2.826
Bis(3-chloropropyl)sulfide		3.512
Ethyl(2-chloroethyl)disulfide		2.828
Diethyl n-butylmalonate		3.495
2-Chloroethylphenylsulfide		3.420
4-Chlorobutyl acetate		2.584
3-Chloropropan-1-ol		1.831
1-Chlorobutane	1.650	1.313
1-Chloropentane	1.975	1.713
1,1,2,2-Tetrabromoethane		3.156
Dibutylether	2.384	2.052
Diisibutylether		1.818
Heptan-2-one	2.417	2.088
Heptan-3-one	2.406	2.065
Nonan-2-one	3.009	2.713
Nonan-3-one	3.091	2.691
2,6-Dimethylheptan-4-one	2.676	2.364
Decan-2-one	3.451	3.009
Chloroacetone		1.159
Cyclopentanone	2.116	1.733
Cyclohexanone	2.447	2.108
Camphor		2.838
Norcamphor		2.335
Phorone		2.759
Isophorone		2.760
sec-Butyl acetate	1.855	3.313

tert-Butyl acetate	1.628	1.510
Pentyl acetate	2.420	2.169
Dimethyl glutarate		2.805
Diethyl pimelate		3.890
Dimethyl adipate		3.138
Ethylacetoacetate		2.205
Diethyl carbonate		1.744
Propylene carbonate		2.256
Dimethyl malonate		2.147
Diethyl malonate		2.604
Diethyl methylmalonate		2.704
Diethyl ethylmalonate		2.941
Dimethyl chloromalonate		2.541
Diethyl chloromalonate		2.965
Methyl trifluoroacetate		0.752
Ethyl trifluoroacetate		1.037
Isopropyl trifluoroacetate		1.037
Ethyl trichloroacetate		2.366
Methyl cyanoacetate		1.965
Ethyl cyanoacetate		2.183
Dimethylaminoacetonitrile		1.639
Dimethylformamide	2.183	1.703
Dimethylacetamide	2.417	1.982
Dimethylsulfoxide	2.457	1.899
Trimethyl phosphate		2.146
Triethyl phosphate	3.073	2.756
Dimethyl methylphosphonate		2.007
c-4-Acetyl-4-n-Pr-cy-hexylamine		4.030
t-4-Acetyl-4-n-Pr-cy-hexylamine		4.052
Heptan-1-ol	2.670	2.334
Octan-1-ol	3.018	2.667
Octan-2-ol	2.810	2.427
Decan-1-ol	3.722	3.282
Cyclohexanol	2.378	2.072
Cyclooctanol	3.361	2.846
Menthol		2.947
2,2,2-Trifluoroethanol		0.794
Hexafluoropropan-2-ol		1.037
2-Chloroethanol		1.384
2-Bromoethanol		1.626
Geraniol		3.214
Benzene	1.639	1.467
Toluene	2.130	1.768
Ethylbenzene	2.468	2.044
n-Propylbenzene	2.785	2.318
1,2,3-Trimethylbenzene	3.077	2.537
1,3,5-Trimethylbenzene	2.901	2.369
3-Ethyltoluene	2.825	2.346
n-Butylbenzene	3.149	2.624
tert-Butylbenzene	2.893	2.435
1,2,3,4-Tetramethylbenzene	3.526	2.903
1-Phenylhexane	3.832	2.232
1,3-Dichlorobenzene	3.028	2.456
3-Chlorotoluene	2.825	2.299
4-Chlorotoluene	2.843	2.320
3-Bromotoluene		2.558
4-Bromotoluene	3.166	2.574

Iodobenzene	3.156	2.531
1-Bromo-2-fluorobenzene		2.270
1-Bromo-3-fluorobenzene		2.179
1-Bromo-2-chlorobenzene		2.774
1-Bromo-3-chlorobenzene		2.700
1-Bromo-4-chlorobenzene		2.709
1-Chloro-2-iodobenzene		3.077
1-Chloro-3-iodobenzene		3.015
1-Chloro-4-iodobenzene		3.027
1-Bromo-2-iodobenzene		3.332
1-Bromo-4-iodobenzene		3.274
Methylphenylether	2.609	2.169
1,3-Dimethoxybenzene	3.438	
Pentafluoroanisole		2.250
Thioanisole		2.659
Methylphenylketone	3.076	2.590
2-Methylacetophenone		2.587
3-Methoxyacetophenone		3.271
Propiophenone	3.410	2.885
Methylbenzylketone		2.771
Methyl benzoate	3.155	2.709
Phenol	2.873	2.349
m-Cresol	3.211	2.644
2,4,6-Trimethylphenol	3.649	3.034
3-Ethylphenol	3.486	2.944
2-Isopropylphenol	3.593	3.048
3-Isopropylphenol	3.693	2.238
4-Fluorophenol	3.017	2.430
2-Chlorophenol	2.936	2.402
4-Chloro-3-methylphenol	4.102	3.302
2,6-Difluorophenol		2.180
2,6-Dichlorophenol		2.491
Methyl salicylate		2.987
Benzyl alcohol	2.935	2.512
Pyridine	1.929	1.646
3-Ethylpyridine	2.764	2.288
2-Methoxypyridine	2.490	2.081
2-Dimethylaminopyridine		2.708
Nicotine		3.425

For many of the compounds in Tables 14-16, the π_2^H and $\Sigma\alpha_2^H$ descriptors are not available, but the determined logL values will be useful in the future, as we obtain the other descriptors. One method of calculating descriptors is through the alternative eq(2), and we will pursue this method in future work. At present, we were able to obtain descriptors for a number of important compounds for which $\Sigma\alpha_2^H$ is zero. These include malonates, sulfides, and some other esters as well. In Table 17 are given the $\log L^{16}$ values that we have obtained from data on the capillary and packed columns, via eq(57)-eq(60), together with the final suggested value, and in Table 18 are the complete set of descriptors for the compounds; note that $\Sigma\alpha_2^H$ is zero for all compounds in Table 18.

Now that all the descriptors are available for the malonates, sulfides, etc., it is possible to use already known equations based on eq(1) and eq(2) to estimate a variety of physicochemical and biological data. Gas-water partition coefficients (or Henry's constants) at 298K can be calculated from equations already listed [25], and a wide variety of water-solvent partition coefficients can be calculated from eq(2), details of which have been published in the literature [6,7]. Equations are to hand [26,27] for the solubility of vapors in a variety of solvents, and in a number of phases of potential use in chemical sensors [28]. It is therefore possible to estimate the detection limit of the malonates and the sulfides with sensors such as SAW devices as the analytical method.

Table 17. Calculated values of $\log L^{16}$ and the average taken

Compound	AP.pack 423	AP.cap 423	AP.cap 353	PDMS 353	Log L^{16}
Chloroacetone		3.497	2.550	2.161	2.356
Diethyl carbonate		2.855	3.081	3.064	3.073
Propylene carbonate	3.980	3.935	3.708	3.976	3.964
sec.Butyl acetate	3.006	3.565	3.081		3.043
tert.Butyl acetate	2.652	3.494	2.774	2.890	2.772
Ethylacetoacetate	3.263	3.575	3.728	3.957	3.754
Dimethyl malonate	3.587	3.305	3.561	3.856	3.577
Diethyl malonate	4.239	4.169	4.254	4.618	4.221
Diethyl methylmalonate	4.334	4.332	4.408	4.784	4.358
Diethyl ethylmalonate	4.731	4.875	4.773	5.184	4.793
Diethyl n-butylmalonate	5.582	5.766	5.692	6.112	5.680
Dimethyl gluterate		4.670	4.554	4.845	4.612
Dimethyl adipate		5.190	5.132	5.396	5.161
Diethyl pimelate		6.482	6.242	6.639	6.455
Dimethyl chloromalonate		4.048			4.048
Diethyl chloromalonate		6.233			6.233
Methyl trifluoroacetate				1.576	1.576
Ethyl trifluoroacetate		2.315		2.051	2.183
Ethyl trichloroacetate	4.083	4.006	4.068	4.276	4.052
4-Chlorobutyl acetate	4.357	4.411	4.358	4.532	4.376
2-Chloroethylmethylsulfide	3.576	3.395	3.578	3.614	3.589
2-Chloroethylethylsulfide	3.993	3.871	4.010	3.972	3.962
2-Chloroethyl-n-propylsulfide	4.441	4.390	4.453	4.474	4.439
2-Chloroethyl-n-butylsulfide	4.701	4.690	4.728	4.757	4.719
2-Chloroethyl-isoPent-sulfide		5.204	5.238	5.318	5.253
Di-tert.butyl disulfide	4.935	4.856	4.950	5.126	4.914
Ethyl(2-chloroethyl)disulfide	4.931	4.845	4.946	5.048	4.943
Bis(2-chloroethyl)disulfide	5.940	0.994	5.931	6.091	5.989
Trimethyl phosphate	3.917	3.363	3.777	3.816	3.837
Dimethyl methylphosphonate	3.380	2.281	3.765	3.656	3.750

Table 18. Calculated descriptors for solutes[a]

Compound	R_2	π_2^H	$\Sigma\beta_2^H$	$\log L^{16}$
Chloroacetone	0.377	0.90	0.43	2.352
Diethyl carbonate	0.058	1.20	0.65	3.073
Propylene carbonate	0.312	1.20	0.65	3.964
sec.Butyl acetate	0.044	0.57	0.47	3.043
tert.Butyl acetate	0.025	0.54	0.47	2.772
Ethylacetoacetate	0.208	0.83	0.80	3.754
Dimethyl malonate	0.203	0.94	0.80	3.577
Diethyl malonate	0.112	0.94	0.77	4.221
Diethylmethyl malonate	0.056	0.94	0.77	4.358
Diethylethyl malonate	0.038	0.92	0.77	4.793
Diethyl n-butylmalonate	0.006	0.90	0.77	5.680
Dimethyl gluterate	0.177	1.39	0.82	4.612
Dimethyl adipate	0.167	1.41	0.85	5.161
Diethyl pimelate	0.067	1.45	0.90	6.455
Dimethyl chloromalonate	0.293			4.048
Diethyl chloromalonate	0.197			0.197
Methyl trifluoroacetate	-0.143	0.75	0.32	1.576
Ethyl trifluoroacetate	-0.207	0.73	0.30	2.183
Ethyl trichloroacetate	0.365	0.71	0.36	4.052
4-Chlorobutyl acetate	0.262	1.16	0.55	4.376
2-Chloroethylmethylsulfide	0.603	0.62	0.42	3.589
2-Chloroethylethylsulfide	0.575	0.62	0.42	3.962
2-Chloroethyl-n-propylsulfide	0.564	0.62	0.42	4.439
2-Chloroethyl-n-butylsulfide	0.554	0.62	0.42	4.719
2-Chloroethyl-isoPe-sulfide	0.533	0.59	0.42	5.253
Di-tert.butyl disulfide	0.642	0.36	0.53	4.914
Ethyl(2-chloroethyl)disulfide	0.870	0.70	0.37	4.943
Bis(2-chloroethyl)disulfide	1.080	0.82	0.48	5.989
Trimethyl phosphate	0.113	1.10	1.00	3.837
Dimethyl methylphosphonate	0.220	0.80	1.05	3.750

[a] The $\Sigma\alpha_2^H$ descriptor is zero for all compounds in this table.

7. References

[1] M.H.Abraham, *Chem. Soc. Revs.*, 1993, 22, 73.
[2] M.H.Abraham, *Pure Appl. Chem.*, 1993, 65, 2503.
[3] M.H.Abraham, P.L.Grellier and R.A.McGill, *J. Chem. Soc. Perkin Trans. 2*, 1987, 797.
[4] M.H.Abraham and J.C.McGowan, *Chromatographia*, 1987, 23, 243.
[5] P.Havelec and J.G.K.Sevcik, *J. Chromatogr.A*, 1994, 677, 319.
[6] M.H.Abraham, *J. Phys. Org. Chem.*, 1993, 6, 660.
[7] M.H.Abraham, H.S.Chadha, G.S.Whiting and R.C.Mitchell, *J. Pharm. Sci.*, 1994, 83, 1085.
[8] The Pomona Medicinal Chemistry Project.
[9] J.R.Conder and C.L.Young, *Physicochemical Measurement by Gas* Chromatography, John Wiley & Sons, N.Y. & London, 1979.
[10] H.W.Kroto, A.W.Allaf and S.P.Balm, *Chem. Revs.*, 1991, 91, 1213.
[11] R.Taylor and D.R.M.Walton, *Nature (London)*, 1993, 363, 685.
[12] M.H.Abraham and D.P.Walsh, *J. Chromatogr.*, 1992, 627, 294.
[13] R.A.McGill, PhD Thesis, University of Surrey, 1988.
[14] T.F.Bidleman, *Anal. Chem.*, 1985, 56, 2491.
[15] W.T.Foreman and T.F.Bidleman, *J.Chromatogr.*,1985, 330, 203.
[16] TRC Thermodynamic Tables, Texas A and M University System, College Station, Texas.
[17] D.Ambrose, J.H.Ellander, E.B.Lees, C.H.S.Sprake and R.Townsend, *J. Chem. Thermodyn.*, 1975, 7, 453.
[18] M.H.Abraham, *J.Chem.Soc., Faraday Trans.1*, 1984, 80, 153.
[19] D.Ambrose and N.B.Ghiassee, *J. Chem. Thermodyn.*, 1987, 19, 903; 1990, 22, 307.
[20] J.A.Riddick and W.B.Bunger, Organic Solvents, Wiley Interscience, New York, 3rd. edn., 1970.
[21] C.F.Askenas and T.E.Daubert, *J. Chem. Eng. Data*, 1988, 33, 225.
[22] W.J.Shuely, Personal communication.
[23] M.Lenca, *J. Chem. Thermodyn.*, 1990, 22, 473.
[24] R.M.Stephenson and S.Malanowski, Handbook of the Thermodynamics of Organic Compounds, Elsevier, Amsterdam, 1987.
[25] M.H.Abraham, J.Andonian-Haftvan, G.S.Whiting, A.Leo and R.W.Taft, *J. Chem. Soc. Perkin Trans. 2*, 1994, 1777.
[26] M.H.Abraham, J.Andonian-Haftvan, J.P.Osei-Owusu, P. Sakellariou, J.S.Urieta, M.C.Lopez and R.Fuchs, *J. Chem. Soc. Perkin Trans. 2*, 1993, 299.
[27] M.H.Abraham, unpublished work.
[28] M.H.Abraham, J.Andonian-Haftvan, C.M.Du, V.Diart, G.S.Whiting, J.W.Grate and R.A.McGill, *J. Chem. Soc. Perkin Trans. 2*, 1995, 369.